Title
IAOS Bulletin 43

Author
Dillian, Carolyn D., cdillian@coastal.edu

Publication Date
2010-06-15

IAOS

International Association for Obsidian Studies Bulletin

Number 43 **Summer 2010**

CONTENTS

News and Information 1
Notes from the President 2
Obituary: Roger C. Green............................ 5
The Obsidian Hydration Cookbook.............. 6
Provenance of Obsidian from Northwest Iran.... 14
Bodie Hills Obsidian...................................27
Instructions for Authors 40
About the IAOS...................................... 41
Membership Application 42

NEWS AND INFORMATION

New Email for Bulletin Submissions

Carolyn Dillian, IAOS *Bulletin* editor, has a new email address. Submissions of articles, news, and notes can be emailed as a Word file to cdillian@coastal.edu

CONSIDER PUBLISHING IN THE IAOS *BULLETIN*

The *Bulletin* is a twice-yearly publication that reaches a wide audience in the obsidian community. Please review your research notes and consider submitting an article, research update, news, or lab report for publication in the IAOS *Bulletin*. Articles and inquiries can be sent to cdillian@coastal.edu Thank you for your help and support!

CALL FOR NOMINATIONS

We will hold elections for Secretary-Treasurer at the 2011 IAOS Annual Meeting in Sacramento, CA. The IAOS Secretary-Treasurer is responsible for a number of activities related to the organization's business operations, including maintaining the organization's membership list and managing membership renewals and new memberships; coordinating the planning of the IAOS Annual Meeting including meeting logistics, agenda, and notification to members; managing the organization's bank and PayPal accounts and disbursing funds for any IAOS expenditures; and facilitating general communication with all IAOS members. The Secretary-Treasurer is elected to a two-year term and can be re-elected to serve multiple successive terms. If you are interested in running for the IAOS Secretary-Treasurer position, or would like to nominate someone, please contact IAOS President Tristan Carter at stringy@univmail.cis.mcmaster.ca

NOTES FROM THE PRESIDENT

Summer greetings to everyone and thanks once again to everyone for entrusting me with your presidentship. Thanks also to outgoing president Ana Steffen for all her hard work and stable stewardship over the past two years and for helping me to pick up the reins at the SAA's this April. Gratitude is also due to our outgoing Secretary/Treasurer Colby Phillips who has done a stellar job with the Association's finances since 2006, not least establishing our on-line PayPal membership system. The St. Louis meetings saw yet another gathering of the clans, with a number of IAOS members using their work to engage in a variety of debates, not least one of this year's hot topics, the role of archaeometry in North American anthropology, following Killick and Goldberg's *Quiet crisis in American Archaeology* paper in the Jan. 2009 edition of the SAA *Bulletin*.

Also, congratulations are due to two of our newest members, Kyle Freund of the University of South Florida (now McMaster) and Chris M. Oswald of the University of Missouri (and member of MURR's archaeometry lab), both of whom were awarded Student Prizes of 2 year memberships on the basis of their high quality poster presentations at the SAA's. The posters are included on the next two pages (click to expand detail).

One of the major points of discussion in our committee meeting this year was increasing membership, not only in North America (where the bulk of our members are based), but also worldwide. To this end we shall be gathering our resources in an IAOS sponsored panel at the Sacramento meetings (March 30th-April 3rd, 2011), where we aim to present to a general SAA audience a state-of-play review of our methodological capabilities (characterization and dating), together with a series of global case studies that showcase how our work is contributing to some of the major debates in anthropological archaeology. Studies on obsidian from Anatolia, the Andes, California, the Pacific, the Rift Valley and the Southwest, will variously be employed to engage with such issues as: early hominin cognition, Neolithisation, material culture and identity, trade and power, plus communities of practice. It should be a great panel; we will make sure you all know the date, time and venue when organized and thereafter encourage you to spread the word! Nothing certain yet, but we are also exploring the possibility of a half-day trip to a northern Californian source and winery, a great way for the membership to interact in the field and hopefully meet some local experts and enjoy some local viticulture (categorically post-obsidian, says he with a nod to the health and safety executive...). As a means of further expanding our engagement with non-US based scholars, we would ultimately aim to sponsor a similar panel at a forthcoming annual meeting of the *European Association of Archaeologists*.

Aside from the IAOS annual meeting at the SAA's, a number of us also had the opportunity to reconvene at the May 2010 bi-annual symposium of the *International Society of Archaeometry*, a hugely successful conference hosted by our own Prof. Rob Tykot. The IAOS was a proud co-sponsor of this event, an investment that also of course helped to raise our profile, leading to a number of new members joining, including scholars from Armenia, Austria and Poland. Here too obsidian studies played a major role, with oral presentations and posters documenting new geo-prospection projects and characterization studies from Armenia, Mexico, Peru, Sardinia, Turkey and the US.

I shall leave you here and wish you all well for your summer fieldwork and continuing good health and productivity. In a few days time I shall be making my annual pilgrimage to Çatalhöyük, where I shall be training two undergraduates in our lithic analysis system and involving them in our visual characterization project. After that, three weeks of visiting the major sources of Eastern and Central Anatolia, followed by those of the Aegean, collecting geological samples for my new McMaster Archaeological XRF Lab [MAX Lab] that should be operational for characterization studies this fall; but more on that next issue...

All the very best

Tristan Carter
stringy@mcmaster.ca
President IAOS
Assistant Professor, Dept. Anthropology, McMaster University / Director MAX Lab

Obsidian Source Use on the Northern Casas Grandes Frontier

Chris M. Oswald, Jeffrey R. Ferguson, Todd L. VanPool, and Christine S. VanPool

University of Missouri-Columbia

Site Background:

The 76 Draw site is located just south of Deming, New Mexico, and was first identified by Brand (1935) as the most northerly site associated with the Casas Grandes culture. This association is based upon the numerous Casas Grandes polychrome sherds that are scattered across the site. The site is also on the periphery of the Salado cultural area, and Salado polychrome sherds are found on the site as well. The site has several large habitation mounds, adobe ceremonial mounds, a roasting pit, and numerous obsidian artifacts, which are the focus of this poster.

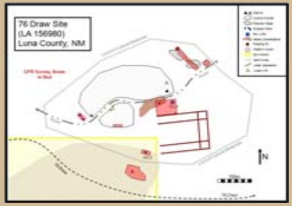

Schematic of the 76 Draw site excavation area.

Photograph of the 76 Draw site excavation during the 2009 field season.

Relationship with Casas Grandes

While the site attributes mentioned above appear to confirm a relationship with the Casas Grandes culture, and Paquimé specifically, other researchers might suggest the northern sites like the 76 Draw site were not under political and/or economic control of Paquimé (Whalen and Minnis 2009). Several different models have been proposed concerning the organization of the Casas Grandes culture. Whalen and Minnis argue that Paquimé's economic and political influence was focused primarily in a "core" zone within 30 km of the site, and was quite limited in "peripheral" sites beyond 60 km. Instead, they suggest such settlements are generally poorly integrated with surrounding sites and the more distant core. Others focus on the Casas Grandes system as a religious/political organization, with Paquimé acting as the religious center that culturally integrated sites throughout the region (Fish and Fish 1999; Schaafsma and Riley 1999; VanPool and VanPool 2009). Because of the demonstrated utility of X-ray florescence in sourcing archaeological materials, an in-depth analysis of the obsidian artifacts recovered from the 76 Draw site should demonstrate the economic relationship among settlements in the periphery.

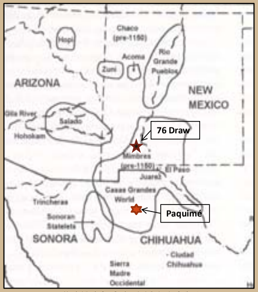

Map depicting the Casas Grandes region in the American Southwest.

Ramos Polychrome. Courtesy of El Paso Museum of Archaeology (Catalogue No. 59-9-197). Photograph by C. VanPool.

Ramos polychrome sherds recovered from the 76 Draw site.

Abstract:

The 76 Draw site represents the northern-most expression of the Casas Grandes culture. This association is evidenced by the numerous Medio period (AD 1200-1450) ceramics recovered from the site. Obsidian artifacts collected from the site during the 2009 summer field season have been chemically analyzed using non-destructive X-ray fluorescence spectroscopy (XRF). This study demonstrates that obsidian procurement further confirms the relationship between the 76 Draw site and the core Casas Grandes cultural region located further south in Chihuahua, Mexico.

Photograph of obsidian debitage collected at the 76 Draw site.

Picture of the handheld Bruker XRF and associated computer spectra.

Why Obsidian Provenance Analysis

X-ray florescence (XRF) was used to determine the source areas of the obsidian artifacts that were recovered from the 76 Draw site. This sourcing technique was chosen because of its non-destructive approach to chemical sourcing, its affordability, and finally because of its successful application in distinguishing obsidian sources in the Southwest.

XRF Methodology

The Bruker Tracer III-V XRF is a handheld portable unit. The instrument has a rhodium-based X-ray tube which operates at 40 kV and a thermoelectrically-cooled silicon detector. The obsidian calibration uses 45 well-known obsidian sources with data from previous XRF and neutron activation analysis (NAA) measurements. The samples were counted for three minutes to measure the minor and trace elements present. The elements reliably measured include Mn, Fe, Th, Rb, Sr, Y, Zr, and Nb. The results were compared to extensive source sample collections for all known sources in the American Southwest.

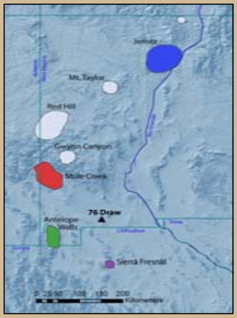

Map of New Mexico showing site and obsidian source locations. Colors of sources correspond with colors in tables.

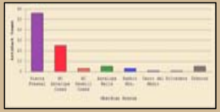

Table depicting the frequency of artifacts assigned to specific obsidian sources.

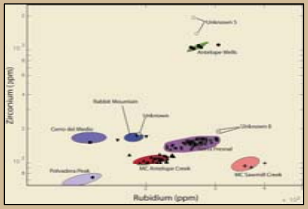

Bivariate plot of the obsidian sources present at the site.

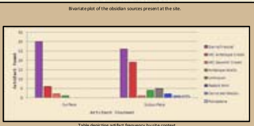

Table depicting artifact frequency by site context.

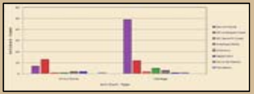

Table depicting the number of artifacts by tool type.

Sampling and Results:

A total of 99 obsidian artifacts were collect during the 2009 field season from the 76 Draw from both surface and excavated contexts. The XRF analysis of these artifacts revealed that 57 percent of the artifacts in the obsidian assemblage are from the Sierra Fresnal source situated in northern Mexico along the banks of the Nuevo Casas Grandes River (Shackley 2005). The second largest source assignment consists of artifacts from the Mule Creek sources with 25 percent from the Antelope Creek sub-source, and another three percent from the Sawmill Creek sub-source. Additional artifacts were assigned to Antelope Wells, and three sources in the Jemez Mountains (Polvadera, Rabbit Mountain, and Cerro del Medio). Five artifacts remain unassigned.

Of the Sierra Fresnal samples only 14 percent of the artifacts are projectile points, whereas for all the other sources combined that number increases to 83 percent. The majority of the artifacts from the Sierra Fresnal source consist of debitage that is believed to be representative of expedient tool production. It is unclear as to why this stark difference in artifact form occurs specifically with the Sierra Fresnal source, but it is likely that this is due to the small size of the original source material that did not generally permit projectile point manufacture. Finally, the analysis regarding obsidian context demonstrates that there is greater variability in obsidian sources represented in the subsurface materials than from surface contexts.

Conclusion:

The majority of the obsidian artifacts recovered from the 76 Draw site are assigned to the Sierra Fresnal source in northern Mexico. The ceramic evidence from 76 Draw, combined with the proximity of the Sierra Fresnal source to the site of Paquimé suggests some form of economic interaction between the two sites. It is uncertain at this point whether this reflects direct trade with Paquimé, down the line trading, or some other form of acquisition.

The majority of the artifacts from the Sierra Fresnal source consist of non-formal tools which may indicate that the source material was too small to fabricate into projectile points, or that the lithic reduction at the site was not focused on bifacial technology. It is clear, however, that there was an emphasis on hunting at the site due to the large amount of faunal remains and projectile points from other obsidian sources found at the site. The site's inhabitants obtained raw materials from a wide area, as evidenced by the presence of a projectile point made from Cerro del Medio obsidian, a source located over 450 km to the north. However, the dominant raw material source for obsidian was to the south, supporting the hypothesis that the northern most site of the Casas Grandes region was more economically integrated with the core area than to other culture areas to the north.

Future Research:

In order to further understand the variability in obsidian source usage by the site's inhabitants, more samples will need to be analyzed from ongoing fieldwork, particularly from subsurface contexts. Furthermore, as we learn more about the stratigraphic nature of the site, future analysis might reveal how obsidian source usage may have changed through time. This analysis coupled with a more detailed focus of the lithic technology will assist in the interpretation of the role of obsidian in regards to the larger stone tool assemblage at 76 Draw. Finally, the continued search for smaller obsidian sources in the region may help account for the unassigned samples encountered during this study.

References Cited:

Brand, Donald D.
1935 The Distribution of Pottery Types in Northwestern Mexico. *American Anthropologist* 37:287-305.
Fish, Paul, and Suzanne K. Fish
1999 Reflections on the Casas Grandes Regional System from the Northwestern Periphery. In *The Casas Grandes World,* edited by Curtis F. Schaafsma and Carroll L. Riley, pp. 27–42. University of Utah Press, Salt Lake City.
Schaafsma , Curtis F. and Carroll L. Riley
1999 The Casas Grandes World. University of Utah Press.
Shackley, Steven M.
2005 Obsidian: Geology and Archaeology in the North American Southwest. University of Arizona Press.
VanPool, Christine S., and Todd L. VanPool
2007 *Signs of the Casas Grandes Shamans.* University of Utah Press, Salt Lake City.
Whalen, Michael E., and Paul E. Minnis
2009 The Neighbors of Casas Grandes: Medio Period Communities of Northwestern Chihuahua. University of Arizona Press.

Acknowledgements:

We would like to thank the owners of the 76 Draw site: The Perez family. Steve Shackley assisted with the identification of the Sierra Fresnal obsidian source and graciously analyzed a few of the samples. Funding support for the XRF analysis was provided by the National Science Foundation (BCS-0802757).

Lithic Technology and Obsidian Exchange Networks in Bronze Age Nuragic Sardinia (Italy)

Kyle P. Freund[1] *& Robert H. Tykot*[2]*, Department of Anthropology, University of South Florida*

Introduction

Sardinia is located in the Mediterranean Sea off the western coast of Italy and occupies an area of approximately 24,000 square kilometers (**Figure 1**). The Sardinian Bronze Age Nuragic period (ca. 1600-850 B.C.) is named after the approximately 7,000 truncated cone-shaped residential stone structures called *nuraghi* which are found throughout the island. The Sardinian Bronze Age (Nuragic period) and the factors which created and maintained an island-wide identity as seen through the presence of its distinctive nuraghi have received considerable attention; however the amount of research directly related to the stone tools of the era has been relatively limited despite the wealth of knowledge it is capable of yielding. This research hopes to contribute to Sardinian archaeology through the study of ancient technology, specifically obsidian lithic technology, by combining typological information with source data gleaned from the use of X-ray fluorescence spectrometry (XRF). This study specifically tests whether changes in the composition of lithic assemblages was accompanied with corresponding changes in how the obsidian was used.

Sites

Monte Arci

Monte Arci is a region in west-central Sardinia which contains the obsidian raw material used for stone tools from the beginning of the Neolithic period and continuing into the Nuragic era. Researchers have identified four subsources located in the Monte Arci area (**Figure 1**) and include SA, SB1, SB2, and SC (Tykot 1997; Luglié et al. 2006). Secondary SC obsidian deposits have also been identified by Luglié et al. (2006) south of the main SC conglomerate.

Marghine Region

Duos Nuraghes

The west-central Sardinian site of Duos Nuraghes (**Figure 1**) is located in the Marghine region on a low knoll in the Borore locale at 400 m elevation (Webster 1996). It typifies a little-studied but important element of Nuragic culture, a Nuragic village. Occupation at the site spanned from ca. 1600 B.C.–A.D. 1000.

Additional Marghine Region Sites

Additional sites in the Borore locale have also been included. They are Nuraghe Urpes, Nuraghe San Sergio, and Nuraghe Serbine. Of these three sites, only at Nuraghe Urpes has there been excavation conducted outside of the nuraghe, hence these sites do not exemplify a representative sample like that of Duos Nuraghes. Nonetheless, they provide a comparative sample from which interpretations can be made.

Ortu Còmidu

The excavation of Nuraghe Ortu Còmidu, located near the Pixina River, south of Monte Arci in the province of Cagliari, took place in 1975, 1976, and 1978 as part of a project which explored early Sardinian metal working (Balmuth and Phillips 1986). Ortu Còmidu likely dates to the early phase of the Nuragic period and is a "complex" nuraghe 12 m in diameter. The site has a central tower, a courtyard with a well, and at least three subsidiary towers attached to the central one (Balmuth and Phillips 1986).

Fig. 1. Map of Relevant Sites

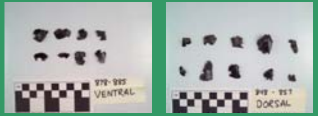

Fig. 2. Some examples of Nuragic obsidian artifacts from Duos Nuraghes

Fig. 3. A Bruker Tracer III-V portable XRF machine

Methods

For this study, a Bruker Tracer III-V portable XRF machine (**Figure 3**) was used to source 344 obsidian artifacts from the Marghine region: 242 from Duos Nuraghes and 102 from Nuraghe San Sergio, Nuraghe Serbine, and Nuraghe Urpes. An additional 144 artifacts from Ortu Còmidu were also sourced. These artifacts were analyzed with the permission of the archaeological superintendency of Sardinia, in the archaeological lab on the University of South Florida campus during the spring of 2009.

A total of 413 obsidian artifacts were also classed into types and then analyzed. This included 228 artifacts from Duos Nuraghes and 71 from the other sites in the Marghine region. An additional 114 artifacts from Ortu Còmidu were classified. It must be pointed out that the number of artifacts which were chemically sourced is larger than the number of artifacts being typologically analyzed. This is due to the fact that some artifacts were too destroyed to be properly measured as a result of undergoing obsidian hydration dating. This destruction may have prohibited a typological analysis, but it did not preclude analysis using XRF.

The process of debitage analysis described by Sullivan and Rozen (1985) has been utilized to classify the artifacts. The crucial conceptual power of this typology is the ability to distinguish between core reduction and tool production based on the varying proportions of debitage categories, thus allowing comparisons to be formulated. Tool production refers to the manufacture of tools through flaking, while core reduction refers to the process of flake removal for the purpose of the acquisition of the detached pieces (Andrefsky 2009:66). Tool production is recognized archaeologically by the presence of a large percentage of broken flakes and flake fragments compared to the number of cores and complete flakes. The inverse is true of core reduction (Sullivan and Rozen 1985). Assemblages were divided into several categories: retouched tools, proximal flakes, medial flakes, distal flakes, and angular waste. One will note that the debitage categories are slightly different than those outlined by Sullivan and Rozen (1985), and further classify flake fragments into medial and distal categories (**Figure 4**). Broken flakes are classified as proximal flakes, thus allowing for additional analyses which can account for post-depositional processes such as flake breakage as a result of trampling.

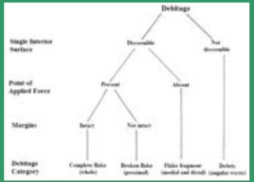

Fig. 4. Debitage classification scheme (adapted from Sullivan and Rozen 1985:759)

Results

Overall, the pattern of obsidian acquisition is roughly similar at all of the observed sites. Type SC obsidian overshadows other subsources in the composition of these Nuragic assemblages. Type SB1 and SB2 were not a significant source of raw material at all, while type SA is the second most common, comprising upwards of one-third of an entire site's assemblage. Similar studies on obsidian at other Nuragic sites carried out by Michels et al. (1984) support these findings (**Figure 5**), but one must note the low number of artifacts sourced at these other sites.

Core reduction seems to be the preferred reduction strategy at all of the sites, with complete flakes making up an average of 40 percent of the assemblages (**Figure 6**). The relatively low number of cores may also indicate that primary reduction occurred at the quarry site or else depositional processes such as the throwing out of used cores may have affected the makeup of the assemblages.

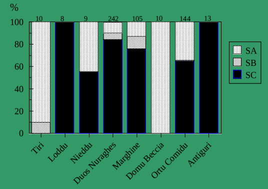

Fig. 5. Obsidian source distribution at other Nuragic sites (adapted from Michaels et al. 1984)

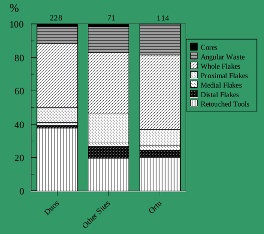

Fig. 6. The distribution of artifacts at all sites

Conclusions

The sourcing and typological analysis consisted of an examination of obsidian lithic artifacts from five Nuragic (ca. 1600-850 B.C.) sites on the island of Sardinia. The geological sources of these artifacts were determined using XRF technology, with the results showing that the SC subsource was the dominant obsidian type which comprised all of the assemblages. This pattern of acquisition has its roots in the Late Neolithic and Chalcolithic time periods, when it is likely that part-time workshops began to emerge which were capable of supplying the entire island with raw materials through down-the-line exchange. It is possible that emerging elites used this increased control of access to obsidian as a means of solidifying and reifying their power.

Typological analysis was used to test whether this change in the composition of lithic assemblages was accompanied with corresponding changes in how the obsidian was used. During the Nuragic, blade technology greatly diminished as assemblages became dominated by the presence of backed lunates and expediently produced unshaped tools. Core reduction strategies were utilized as cores were flaked and the resulting debitage was selected for and further reduced according to the immediate needs. These unspecialized tools were used for a wide range of activities, which is seen in the high degree of variability in the retouch locations and angles. Slight typological differences were evident across the island, but this could be due to the lack of comprehensive excavations conducted at sites other than Duos Nuraghes. In general however, Nuragic lithic technology is similar at all of the studied sites. It is therefore possible to accept the null hypothesis which states that changes in the acquisition of obsidian raw materials during the Chalcolithic and Nuragic in Sardinia are coupled with corresponding changes in how the obsidian was used.

References

Andrefsky, W., Jr.
2009 The analysis of stone tool procurement, production, and maintenance. *Journal of Archaeological Research* 17:65-103.

Balmuth, M.S., and P. Phillips
1986 Sardara (Cagliari): preliminary report of excavations 1975-1978 of the Nuraghe Ortu Còmidu. *Notizie degli Scavi di Antichita* 37:353-372.

Luglié, C., F-X. Le Bourdonnec, G. Poupeau, M. Bohn, S. Meloni, M. Oddone, and G. Tanda
2006 A map of the Monte Arci (Sardinia island, Western Mediterranean) obsidian primary to secondary sources. Implications for Neolithic provenance studies. *Comptes Rendus Palevol* 5:995-1003.

Michels, J.W., E. Atzeni, I.S.T. Song, and G.A. Smith
1984 Obsidian hydration dating in Sardinia. In *Studies in Sardinian Archaeology*, edited by M.S. Balmuth and R.J. Rowland, Jr., pp. 83-114. The University of Michigan Press, Ann Arbor.

Sullivan, A.P., III, and K.C. Rozen
1985 Debitage analysis and archaeological interpretation. *American Antiquity* 50(4):755-779.

Tykot, R.H.
1997 Characterization of the Monte Arci (Sardinia) obsidian sources. *Journal of Archaeological Science* 24:467-479.

Webster, G.S.
1996 *A Prehistory of Sardinia 2300-500 B.C.* Sheffield Academic Press, Sheffield.

1Department of Anthropology, University of South Florida Email: kpfreund@mail.usf.edu
2Department of Anthropology, University of South Florida Email: rtykot@usf.edu

OBITUARY: ROGER CURTIS GREEN, IAOS Board of Advisors
(March 15, 1932 - October 4, 2009)
For additional tributes, please see: http://www.nzarchaeology.org/Roger.html

The following obituary was written for the University of Auckland *News* website by Peter Sheppard, Associate Professor in Archaeology who came to New Zealand as a Post-doctoral Scholar to work with Roger on aspects of the archaeology of the Solomon Islands.

In 1958 archaeologist Roger Green came to the University of Auckland as a Fullbright scholar to spend 9 months in New Zealand preparing for fieldwork in French Polynesia. Although Roger's early interest was the archaeology of the southwest USA, his exposure at Harvard to the Pacific anthropologist Douglas Oliver turned his interest to the Pacific. This shift in interest resulted in a career which spanned 50 years and field research which covered Oceania.

In 1961 Roger joined the Department of Anthropology at Auckland as the only archaeologist, replacing Professor Jack Golson, who had moved to ANU. Between 1961 and 1967 Roger conducted significant research in New Zealand, ultimately writing the important theoretical piece *A Review of the Prehistoric Sequence in the Auckland Province*, which was presented as his Harvard PhD. In keeping with his life-long pattern, however, his New Zealand research was complemented by large seminal research projects in the tropical Pacific (Moorea 1961-62; Western Samoa 1963-1967).

These projects were funded by the NSF through the Bishop Museum in Hawaii and in 1967 Roger left Auckland to take up a position at the Bishop. During this period (1967 to early 1970) Roger conducted important work on a series of Hawaiian valley systems, where he initiated research into agricultural field systems in collaboration with the New Zealand born ethnobotanist Douglas Yen.

Roger returned to Auckland in 1970 as the first James Cook Fellow, taking up a three year position at the Auckland Museum. From the Museum he initiated, with Douglas Yen, the Southeast Solomons Culture History Project (1970-72, 1976). This was the first large-scale, multi-disciplinary, multi-phase archaeological research project in the Pacific and the breadth of collaboration amongst archaeologists, social anthropologists, linguists, geologists, palynologists and other archaeological scientists reflected Roger's enduring interest in what he termed 'holistic archaeology or anthropological history'.

During this project sites bearing Lapita pottery were found in the Reef/Santa Cruz Islands which lie 400km beyond the Main Solomons across what Roger came to call the Near/Remote Oceania boundary. This boundary marked the limits of human settlement until people bearing Lapita culture and speaking Austronesian languages moved out into the Pacific some 3,200 years ago. Although Lapita sites had been found prior to Roger's work, his were the first systematic excavations providing detailed information on the Lapita culture and as such they have served as archetypes for subsequent work and debate. Throughout the rest of his career questions of Lapita settlement and Polynesian origins were at the core of Roger's work and he continued to publish on his Southeast Solomons research up until his death.

In 1973 Roger was appointed to a personal Chair at Auckland which he held until his retirement in 1992, after which he was Emeritus until his death. Retirement for Roger simply meant more opportunity for publishing and his output has been prodigious. In 1995 at the time of the publication of the festschrift, *Oceanic Culture History: Essays in Honour of Roger Green*, a bibliography of 259 publications was compiled. Since 1995 publication has been steady with two new papers in the week prior to his death and more in train. Perhaps one of Roger's proudest achievements in later years was his co-authoring with Professor Patrick Kirch (University of California, Berkeley) in 2001 of *Hawaiki, Ancestral Polynesia: An Essay in Historical Anthropology*, which allowed him to combine his expertise in Pacific archaeology and linguistics and provide a theoretical and methodological basis for a holistic historical anthropology.

Roger Green has been a foundation scholar in the archaeology of the Pacific and his contribution is marked by his publication record but also by his hundreds of colleagues and students who have gone on to define the field. His contributions were recognized by memberships in the National Academy of Science (USA) and the Royal Society of New Zealand. In 2003 he was awarded the Marsden Medal by the New Zealand Association of Scientists for his work in Pacific archaeology and cultural history and in 2007 he was made an Officer of the New Zealand Order of Merit (ONZM) for 'services to New Zealand history'. Roger has been the father and grandfather of archaeology and anthropology at the University of Auckland, his academic family will miss him. *Kua hinga te kauri o te wao nui a Tāne*

Roger Curtis Green 1932–2009 BA BSc (New Mexico) PhD (Harvard) ONZM FRSNZ Member NatAcadSci (USA), Hon Fellow Society of Antiquaries of London Emeritus Professor of Prehistory at the University of Auckland

---

THE OBSIDIAN HYDRATION COOK BOOK: AID FOR THE MATHEMATICALLY DISINCLINED

Alexander K. Rogers, MA, MS
Archaeology Curator and Staff Archaeologist
Maturango Museum

Abstract

This paper describes a simple procedure for obsidian hydration dating. It is based on the specific case of Coso obsidian from sites with a desert temperature regime, but can be extended to other areas and to obsidian from other sources by modifying the temperature model and using the appropriate hydration rate parameters. The process corrects hydration rim values for effective hydration temperature (EHT) and computes age estimates, using a rate equation based on radiocarbon-obsidian pairings for Coso obsidian. A correction for paleoclimatic change is included. The analysis can be performed by Excel spread sheet or scientific calculator; for larger jobs, program listings in MatLab are provided to expedite the process. References are cited which show how to compute hydration rate and site temperature parameters, in the event that the user needs to analyze other obsidians and other temperature regimes.

Introduction

This paper describes a protocol for obsidian hydration dating, using a hydration rate characteristic of Coso and temperatures typical of the northern Mojave Desert and southwestern Great Basin. The analysis corrects rim values for effective hydration temperature (EHT) and computes age estimates. A correction for paleoclimatic change is described which may be implemented if desired.

It is assumed that the reader is familiar with the techniques of optical measurement of hydration, and the analysis below starts with obsidian hydration rims from a known obsidian source (Coso). The analysis procedure is described first, for those impatient to start, and is followed by a discussion of the theory. The references cited are not exhaustive, but will provide useful background for those interested.

Analysis Procedure

The recommended procedure for chronometric analysis is to proceed by the following steps. All temperatures are in °C; further, rcybp means "radiocarbon years before 1950" and cyb2k means "calibrated years before 2000". An Excel spreadsheet is a convenient way to implement the process.

1. Using the altitude of the site, compute T_a, V_a, and V_d from the equations

$T_a = 22.25 – 1.8h$,

$V_{a0} = 1.65 + 0.94T_a$,

$V_{d0} = 15.8$

If any specimen is from a rock shelter or cave, multiply V_a by 75% and use $V_d = 5°C$.

2. Make sure all the specimens are Coso obsidian.

3. Using the temperature parameters from step 1 and the burial depth z in meters, compute the EHT for each specimen:

$V_a = V_{a0}\exp(-0.44z)$

$V_d = V_{d0}\exp(-8.5z)$

$Y = V_a^2 + V_d^2$

$EHT = T_a\times(1-Y\times3.8\times10^{-5})+.0096\times Y^{0.95}$

Note that the last term in the EHT equation involves raising Y to the 0.95 power. This is easily performed in MS Excel by entering [Y]^.95, where [Y] is the cell reference to the cell containing the Y variable.

4. Compute the EHT-corrected rim thickness for each specimen, using a value of $EHT_r = 20.4°C$.

$RCF = \exp[-0.06(EHT-EHT_r)]$

$r_c = RCF \times r$

5. Group the EHT-corrected rim data as may be appropriate archaeologically; exclude outliers by Chauvenet's theorem (Taylor 1982).

6. Compute ages based on current conditions (k is hydration coefficient):

$t = k\ r^2$

$k = 38.87\ rcybp/\mu^2$

$k = 43.72\ cyb2k/\mu^2$

As an example, consider the case of a Coso obsidian specimen with a 5.0µ rim, retrieved from a surface site at an altitude of 2,440 ft amsl in the northern Mojave Desert. Substituting h = 2.44 in step 1 above gives $T_a = 17.86°C$, $V_a = 18.44°C$, and $V_d = 15.80°C$. Entering these into step 3, with a burial depth z = 0, gives an EHT of 21.57°C. With an EHT_r of 20.4°C, step 4 gives an RCF of 0.9321, so the corrected rim value is 0.9321×5µ = 4.66µ. Finally, using this rim value in step 6 gives ages of 844 rcybp or 950 cyb2k.

7. Consult Figure 1 below to decide whether to make a correction for paleotemperature changes. The figure shows the change in hydration coefficient k due to paleotemperature change as a function of artifact age.

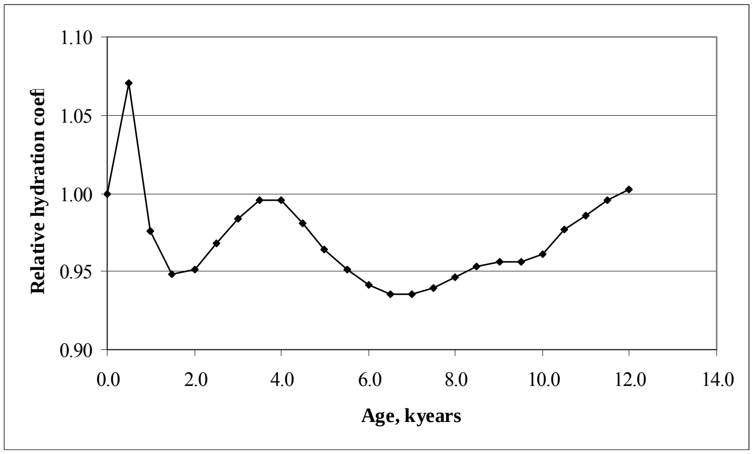

Figure 1. Hydration coefficient relative to present conditions.

The effect of paleotemperature change is especially significant during certain periods: Holocene Maximum around 6,000 years ago, Medieval Climatic Anomaly and Little Ice Age. Use of the present-day hydration rate is not appropriate in these age ranges, whereas for ages about 4,000 years ago the effect is negligible. To apply the correction, compute the age as in step 6. In Fig 1, read off the change in k for that age; multiply k from step 6 by the change, and recompute age. For example, suppose the EHT corrected rim reading is 15µ, which gives an age of 8746 rcybp. The change in k from Fig 1 is about 0.95. Multiply k by this value to give 38.87 × 0.95 = 36.93. Now recompute the age as $36.93 \times 15^2 =$ 8309 rcybp.

8. Once you have the ages, compute the accuracy of the age estimates. First compute the sample standard deviation for each estimate as

$$\sigma_{tr} = 2 \times t \times (\sigma_r / r)$$

where t is the age estimate, r is the mean EHT-corrected rim value, and σ_r is the standard deviation of the rim values for that estimate. Next compute

$$\sigma_{tFlow} = CV_{Flow} \times t$$

where CV_{Flow} is the coefficient of variation of the hydration rate for the particular obsidian flow of interest and t is the age estimate. The values of CV_{Flow} for Coso are in Table 1.

Table 1. Values of CVFlow for Coso Obsidian Sources

Flow Source	**CV_{Flow}**
Sugarloaf Mountain	0.07
West Sugarloaf	0.20
West Cactus Peak	0.25
Joshua Ridge	0.20

If the source is not specified, use $CV_{Flow} = 0.21$ for the Coso Volcanic Field.

Finally, compute the point accuracy of the age estimate by

$$\sigma_a = \sigma_t / \sqrt{N}$$

where σ_t is either σ_{tr} or σ_{tFlow} , whichever is greater. This is the best estimate of accuracy.

9. Finally, the span of time represented by the rim data is either σ_{tr} or σ_{tFlow} , whichever is greater.

You are now ready to do archaeological assessments based on the obsidian data.

Theory

1. Obsidian Hydration

Hydration of obsidian is known as a diffusion-reaction process (Doremus 2002). The basis of chronometric analysis using obsidian hydration is the equation

$$t = k\,r^2 \qquad (1)$$

where t is age in calendar years, r is rim thickness in microns, and k is a constant, the hydration coefficient. Here k is the reciprocal of the hydration rate. Although other equations have been proposed (e.g. Basgall 1991; Pearson 1994), equation 1 is the only form with both theoretical (Ebert et al. 1991; Doremus 2002) and laboratory (Doremus 1994; Stevenson et al. 1998, 2000) support.

The age parameter in equation 1 is in calibrated years before the hydration measurement was made; for analysis purposes this can be taken as the year 2000, so the measurement is in calibrated years before 2000, or cyb2k. When obsidian data are expressed in radiocarbon years before the present (rcybp, by convention referenced to 1950), the quadratic form is still the best fit, giving the smallest overall error in age estimation, but with a different rate constant.

The hydration coefficients for Coso obsidian used herein are

$$k = 38.87\ \text{rcybp}/\mu^2 \qquad (2a)$$

$$k = 43.72\ \text{cyb2k}/\mu^2 \qquad (2b)$$

for rim values

$$0 < r < 12\mu$$

(Rogers 2009).

The hydration coefficient is affected by five parameters: ground-water chemistry (Morgenstein et al. 1999); obsidian anhydrous chemistry (Friedman et al. 1966); obsidian intrinsic water content (Zhang and Behrens 2000); humidity (Mazer et al. 1991); and temperature (Rogers 2007a). Ground-water chemistry is only a problem in cases where potassium content is very high, as in some desert playas; otherwise it can be ignored. Obsidian anhydrous chemistry is controlled by sourcing the obsidian. Intrinsic water concentration can vary within an obsidian source (Stevenson et al. 1993), and can affect hydration rate significantly (Zhang and Behrens 2000); there are no archaeologically appropriate techniques for measuring intrinsic water at present, so its effects must be controlled statistically, by sample size. Humidity is a small effect which can generally be ignored.

Temperature is the major effect which needs to be controlled in performing an obsidian analysis. Archaeological temperatures vary both annually and diurnally, and the hydration rate is a strong function of temperature. The key concept is "effective hydration temperature" (EHT), which is defined as a constant temperature which yields the same hydration results as the actual time-varying temperature over the same period of time. Due to the mathematical form of the dependence of hydration rate on temperature, EHT is always higher than the mean temperature. The mathematical derivation is given in Rogers 2007a.

The equation for EHT, which specifically accounts for average annual temperature, mean annual temperature variation, mean diurnal temperature variation, and burial depth, is

$$\text{EHT} = T_a \times (1 - Y \times 3.8 \times 10^{-5}) + .0096 \times Y^{0.95} \qquad (3)$$

where T_a is annual average temperature, and the variation factor Y for surface artifacts is defined by

$$Y = V_a^2 + V_d^2\,, \qquad (4a)$$

in which V_a is annual temperature variation (July mean minus January mean) and V_d is mean diurnal temperature variation. All temperatures are in degrees C.

For buried artifacts, V_a and V_d represent the temperature variations at the artifact burial depth, which are related to surface conditions by

$$V_a = V_{a0}\exp(-0.44z) \qquad (4b)$$

and

$$V_d = V_{d0}\exp(-8.5z) \qquad (4c)$$

where V_{a0} and V_{d0} represent nominal surface conditions and z is burial depth in meters (Carslaw and Jaeger 1959:81). Depth correction for EHT is desirable, even in the presence of site turbation, because the depth correction, on the average, gives a better age estimate.

Once EHT has been computed, the measured rim thickness is multiplied by a rim correction factor (RCF) to adjust the rims to be comparable to conditions at a reference site:

$$RCF = \exp[-0.06(EHT-EHT_r)] \qquad (5)$$

where EHT_r is effective hydration temperature at the reference site. The EHT-corrected rim value r_c is then

$$r_c = RCF \times r \qquad (6)$$

The value of EHT_r for Coso obsidian is conventionally taken to be that of Lubkin Creek, or CA-INY-30, which is 20.4ºC by this technique. Since most Coso work uses CA-INY-30 as a reference, correcting the rim to these conditions allows direct comparison of EHT-corrected rim data with other published data.

Temperatures have varied slightly over archaeological time scales, which can introduce a small error (<7%) into age estimates made based on current conditions. A technique to correct for this has been described (Rogers 2010), but is generally needed only in Paleoindian studies. A procedure for implementing this calculation is given in Rogers 2010.

2. Temperature Estimation

Most archaeological sites are not collocated with meteorological stations but temperature parameters for them can be estimated by regional temperature scaling (Rogers 2008a). It is important to use long-term data in these computations, and 30 years is the standard for determining climatological norms (Cole 1970). Such data can be down-loaded from the web site of the Western Regional Climate Center. The scaling principle is that desert temperature parameters are a strong function of altitude above mean sea level, and the best estimates of temperature are determined by scaling from 30-year data from large a number of meteorological stations.

With this technique, in the northern Mojave Desert, annual average temperature can be predicted by the equation

$$T_a = 22.25 - 1.8h, \quad 0.94 \le h \le 11.8, \qquad (7)$$

where h is altitude in thousands of feet. The accuracy of this model is 0.98ºC, 1-sigma.

The annual temperature variation can be predicted by

$$V_a = 1.65 + 0.94T_a, \qquad (8)$$

with T_a defined as above. The accuracy of the prediction is 0.27ºC, 1-sigma.

The best fit between V_d and altitude is relatively poor, and, in the absence of other data about a site, the optimal estimate is

$$V_d = 15.8ºC \qquad (9)$$

for locations in the western Great Basin and deserts, irrespective of altitude. The accuracy of this estimate is 1.67ºC, 1-sigma.

These equations are for air temperatures. Obsidian on the surface is exposed to surface temperatures, which can be significantly higher than air temperatures in areas devoid of vegetation (Johnson et al. 2002; Rogers 2008b). However, a detailed analysis based on data from Rose Spring (CA-INY-372) has been shown that meteorological air temperature gives a good estimate of surface ground temperature in situations in which even intermittent shade is present (Rogers 2008c).

3. Paleotemperature Effects

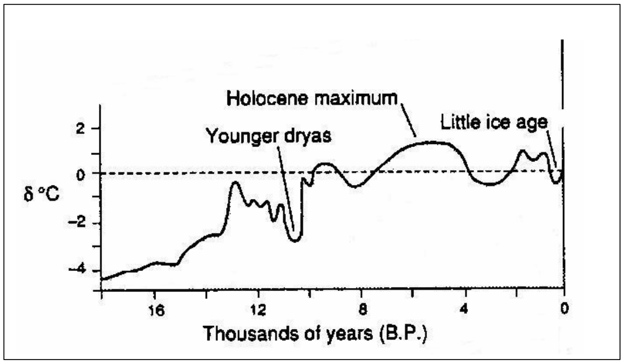

Figure 2. Changes in regional-scale mean temperatures since the late Pleistocene, based on multi-proxy data (West et al. 2007:17, Fig. 2.2)

Since climate has not been stable over periods of archaeological interest, the effects of resulting temperature changes must be included in some cases. Figure 2 shows a reconstruction of the variation of regional-scale mean temperature since the late Pleistocene, based on multi-proxy data (West et al. 2007).

Computation of the effective hydration coefficient for ancient artifacts, including the temperature variations in Figure 2, results in the relative hydration coefficient curve of Figure 1.

Figure 1 shows that temperature changes probably did affect the hydration rate of obsidian throughout the Holocene to a noticeable degree. The effect is especially significant for the Holocene Maximum around 6,000 years ago, and more recently during the Medieval Climatic Anomaly and the Little Ice Age. Use of the present-day hydration rate is not appropriate in these age ranges.

4. Accuracy and Resolution

Age is computed from equation 1, after appropriate temperature corrections. However, in actuality experimental errors occur in both r and k. Errors occur in r because of material inhomogeneities and due to the finite accuracy of laboratory procedures. Errors arise in k due primarily to unpredictable variations in water content in the obsidian (Ambrose and Stevenson 2004; Rogers 2008d; Stevenson et al. 1993, 2000; Zhang et al. 1991; Zhang and Behrens 2000). Since these effects are independent, but cannot be easily separated in practice, it is useful to examine two limiting cases.

The simplest case is to assume that the hydration coefficient k is known and error-free, and all errors are in the measurement of the rim r. For this case it can be shown that the standard deviation in the age estimates due to the standard deviation of errors in r (σ_r) is

$$\sigma_{tr} = 2\times t\times(\sigma_r/r) \qquad (10)$$

This is the familiar sample standard deviation.

For the second case we assume that all error is arising from uncorrected variations in k, which is a function of the individual obsidian flow and has been published for Coso (Stevenson et al. 1993; Rogers 2008d). The standard deviation in age due to such flow-related uncertainties is

$$\sigma_{tFlow} = CV_{Flow} \times t \qquad (12)$$

where CV_{Flow} is the measured uncertainty in hydration rate specific to the flow. Values of CV_{Flow} were presented in Table 1; for the Coso volcanic field as a whole, $CV_{Flow} = 0.21$ (Rogers 2008d).

Finally, the point accuracy σ_a is given by

$$\sigma_a = \sigma_t/\sqrt{N} \qquad (13)$$

where σ_t is either σ_{tr} or σ_{tFlow} , whichever is greater.

Extension of the Method

To apply this method to other obsidian sources, an appropriate hydration coefficient is needed, for known EHT conditions. Obsidian-radiocarbon association is the best method of developing a hydration coefficient; an example of the process can be found in Rogers 2009. Extension to other geographic areas requires a temperature analysis as in Rogers 2008a. The analysis method is the same with these numerical modifications.

Implementation of the Process

The analysis procedure described above can be carried out with a scientific calculator or an Excel spread sheet. Making the correction for paleotemperature changes requires an iterative process, as described above.

For analysis requiring large numbers of computations, however, even the spread sheet becomes cumbersome. For such cases it is convenient to use a computer program to perform the repetitive calculations. Two such programs have been developed, written in MatLab. Program OHAStandard is a demand-response program, suitable for individual data points. Program OHAMatrix is designed for large data sets; it reads input from an Excel-generated comma-separated variable (.csv) input file, and outputs to a similar file. In either case the paleoclimatic correction is made by an iterative fit to the Holocene curve of Fig. 2. Point accuracy and sample standard deviations are computed, and a warning is provided if the calculation is outside the valid range of the equations. These programs may be obtained by contacting the author at matmus1@maturango.org

References Cited

Note: References from the International Association for Obsidian Studies are available to download from their web site, http://members.peak.org/~obsidian/

Basgall, Mark E.

1990 *Hydration Dating of Coso Obsidian: Problems and Prospects*. Paper presented at the 24th Annual Meeting of the Society for California Archaeology, Foster City.

Carslaw, H. S., and J. C. Jaeger

1959 *Conduction of Heat in Solids*, 2nd ed. Oxford: Clarendon Press.

Cole, F. W.

1970 *Introduction to Meteorology*. Wiley: New York.

Doremus, R. H.

1994 *Glass Science*, 2nd. ed. New York: Wiley Interscience.

2000 Diffusion of Water in Rhyolite Glass: Diffusion-reaction Model. *Journal of Non-Crystalline Solids* 261 (1):101-107.

2002 *Diffusion of Reactive Molecules in Solids and Melts*. New York: Wiley Interscience.

Ebert, W. L., R. F. Hoburg, and J. K. Bates

1991 The Sorption of Water on Obsidian and a Nuclear Waste Glass. *Physics and Chemistry of Glasses* 34(4):133-137.

Friedman, Irving, Robert I. Smith, and William D. Long

1966 Hydration of Natural Glass and Formation of Perlite. *Geological Society of America Bulletin* 77:323-328.

Hull, Kathleen L.

2001 Reasserting the Utility of Obsidian Hydration Dating: A Temperature-Dependent Empirical Approach to Practical Temporal Resolution with Archaeological Obsidians. *Journal of Archaeological Science* 28:1025-1040.

Johnson, Michael J., Charles J. Mayers, and Brian J. Andraski

2002 *Selected Micrometeorological and Soil-Moisture Data at Amargosa Desert Research Site in Nye County near Beatty, Nevada, 1998 – 2000.* U.S. Geological Survey Open-File Report 02-348. USGS, Carson City, Nevada. With CD containing meteorological data records.

Mazer, J. J., C. M. Stevenson, W. L. Ebert, and J. K. Bates

1991 The Experimental Hydration of Obsidian as a Function of Relative Humidity and Temperature. *American Antiquity* 56(3):504-513.

Morgenstein, M. E, C. L. Wickett, and A. Barkett

1999 Considerations of Hydration-Rind Dating of Glass Artefacts: Alteration Morphologies and Experimental Evidence of Hydrogeochemical Soil-zone Pore Water Control. *Journal of Archaeological Science*. 26:1193-1210.

Pearson, James L.

1995 *Prehistoric Occupation at Little Lake, Inyo County, California: A definitive Chronology.* Unpublished MA thesis, Department of Anthropology, California State University, Los Angeles.

Rogers, Alexander K.

2007a Effective Hydration Temperature of Obsidian: A Diffusion-Theory Analysis of Time-Dependent Hydration Rates. *Journal of Archaeological Science* 34:656-665.

2008a Regional Scaling for Obsidian Hydration Temperature Correction. *Bulletin of the International Association for Obsidian Studies* 39: 15-23.

2008b Field Data Validation of an Algorithm for Computing Effective Hydration Temperature of Obsidian. *Journal of Archaeological Science.* 35:441-447.

2008c An Evaluation of Obsidian Hydration Dating as a Chronometric Technique, Based on Data from Rose Spring (CA-INY-372), Eastern California. *Bulletin of the International Association for Obsidian Studies,* 40: 12-32.

2009 An Estimate of Coso Obsidian Hydration Rate, Based on Obsidian-Radiocarbon Pairings and the "Weighted Total Least-Squares" Method. *Bulletin of the International Association for Obsidian Studies,* 41: 9-20.

2010 How Did Paleotemperature Change Affect Obsidian Hydration Rates? *Bulletin of the International Association for Obsidian Studies,* 42: 13-20.

Stevenson, Christopher M., E. Knauss, J. J. Mazer, and J. K. Bates

1993 The Homogeneity of Water Content in Obsidian from the Coso Volcanic Field: Implications for Obsidian Hydration Dating. *Geoarchaeology* 8(5):371-384.

Stevenson, Christopher M., J. J. Mazer, and B. E. Scheetz

1998 Laboratory Obsidian Hydration Rates: Theory, Method, and Application. In: *Archaeological Obsidian Studies: Method and Theory. Advances in Archaeological and Museum Science*, Vol. 3, M. S. Shackley, ed., pp.181-204. New York: Plenum Press.

Stevenson, Christopher M., Mike Gottesman, and Michael Macko

2000 Redefining the Working Assumptions for Obsidian Hydration Dating. *Journal of California and Great Basin Anthropology* 22(2):223-236.

Taylor, J. R.

1982 *An Introduction to Error Analysis*. Mill Valley: University Science Books.

Zhang, Y., E. M. Stolper, and G. J. Wasserburg

1991 Diffusion of Water in Rhyolytic Glasses. *Geochimica et Cosmochimica Acta* 55:441-456.

Zhang, Y, and H. Behrens

2000 H_2O Diffusion in Rhyolitic Melts and Glasses. *Chemical Geology* 169:243-262.

PROVENANCE OF OBSIDIAN TOOLS FROM NORTHWESTERN IRAN USING X-RAY FLUORESCENCE ANALYSIS AND NEUTRON ACTIVATION ANALYSIS

Sohila Ghorabi[1], Farhang Khademi Nadooshan[2], Michael D. Glascock[3], Alireza Hejabari Noubari[4], Mansuor Ghorbani[5]

Department of Archaeology, Tarbiat Modares University, Tehran, Iran[1-2-4]
Research Reactor Center, University of Missouri, Columbia, MO, USA[3]
Department of Geology, Shahid Beheshti University, Tehran, Iran[5]

Abstract

In this paper 212 obsidian tools from archaeological sites in northwestern Iran, including the Tabriz: Khodafarin cemeteries, Ardebil: Ghosha Tepe-Shahryi, and Urmia:Dem-i-suliman were analyzed by X-ray Fluorescence Analysis and Neutron Activation Analysis. The aim of the analysis was to determine the provenance of these samples. These sites were chosen for study because of the abundance of obsidian samples on archaeological sites in northwest Iran and their proximity to obsidian sources in Armenia, Azerbaijan, and Turkey. A comparison of the results shows that obsidian trade and exchange between the archaeological sites and sources was quite extensive.

Key words:
Obsidian, northwest Iran, provenance, XRF, NAA

Introduction

Obsidian, with a composition similar to rhyolite, is formed when highly viscous molten lava cools rapidly such that the process of crystallization is precluded. The chemical composition of obsidian at any particular source or flows is, with few exceptions, homogeneous. Different sources or flows are also compositionally different from one another (Glascock *et al.* 1998).

Research on the obsidian provenance which started almost five decades ago has employed a number of chemical methods of analysis:, including: (1) PIXE to study obsidian from New Zealand (Duerden *et al.* 1984); (2) XRF to characterize obsidian from northern California (Hughes 1982); and (3) NAA to analyze obsidian from the highlands of Guatemala (Asaro *et al.*1978).

Renfrew and colleagues, in the mid-1960s, were the first to demonstrate that the chemical compositions of obsidian artifacts could be used to reconstruct obsidian exchange networks involving the Anatolian sources.

In 2009, 212 obsidian samples were analyzed by X-ray fluorescence (XRF) and neutron activation analysis (NAA) at the Archaeometry Lab at MURR. The artifacts came from archaeological sites in northwestern Iran, including Tabriz: Khodafarin cemeteries, Ardebil: Ghosha Tepe-Shahryi, and Urmia: Dem-i-suliman. The objective of the analysis was to determine the compositions of the obsidian artifacts. By comparing the artifact compositional data to compositional data for obsidian sources, it will be possible to study prehistoric trade and exchange of obsidian. The sources most likely to be responsible for obsidian artifacts found in northwestern Iran are located in Armenia, Azerbaijan, Turkey, and Iran.

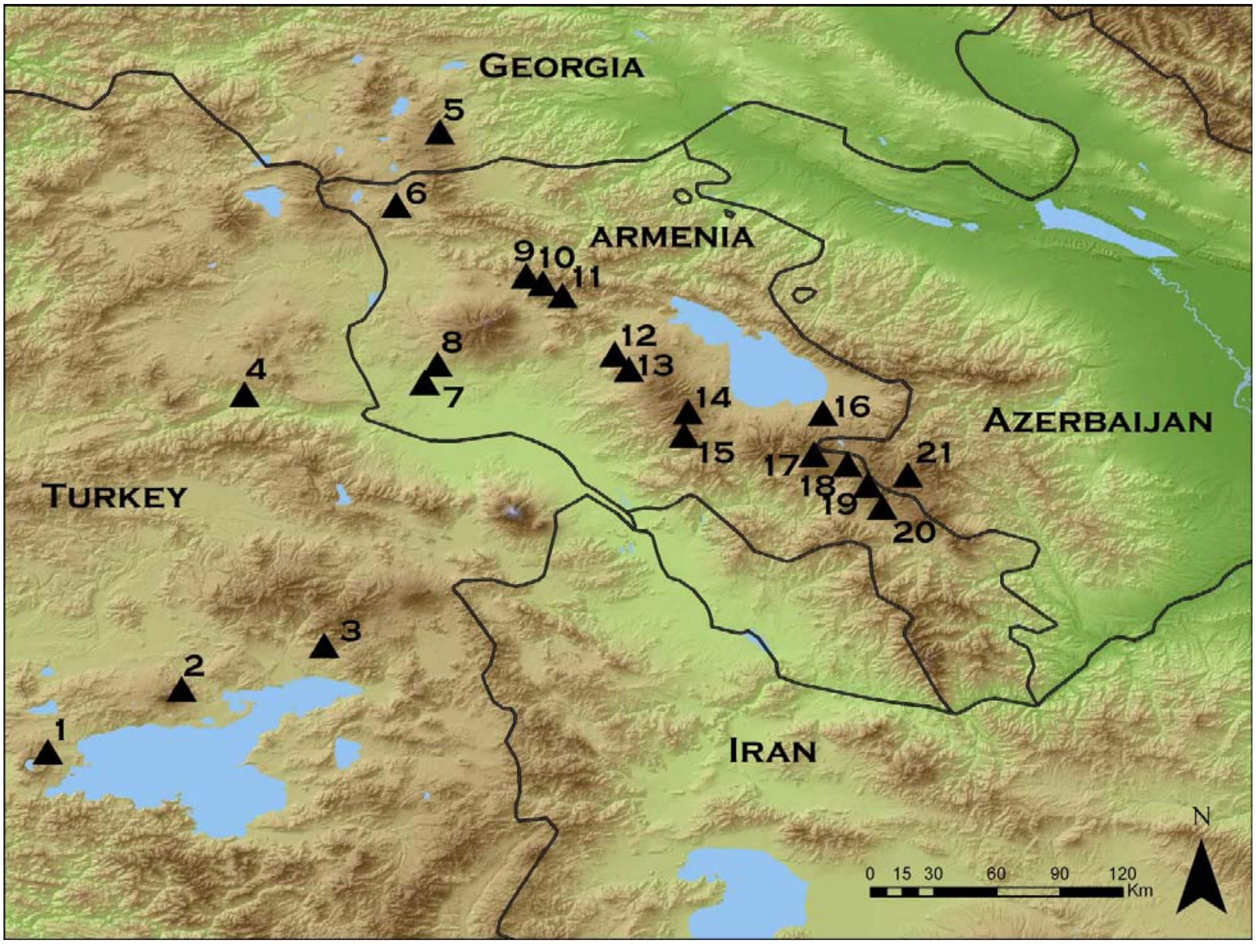

Fig. 1. Map showing locations of obsidian sources from Near East characterized by the Archaeometry Lab at MURR. Source names are as follows: (1) Nemrut; (2) Suphan; (3) Meydan; (4) Sarikamis; (5) Chikiani; (6) Ashotsk; (7) Pokr Arteni; (8) Metz Arteni; (9) Damlik-Hankavan; (10) Tsaghkunyats; (11) Kamakar ; (12) Gutansar; (13) Hatis ; (14) Geghasar; (15) Spitaksar; (16) Vardenis; (17) Choraphor; (18) Satanakar; (19) Sevkar; (20) Bazenk; and (21) Kelbadzhar.

Archaeological Sites of Tabriz, Ardebil, and Urmia

The Khodafarin cemeteries are located near Tabriz in the East Azerbaijan province of Iran in Kaleybar township, including Larijan cemetery is located in 9 km Khomarlu city with 39° 9' 39" longitude and 47° 0' 12" latitude (296 m above sea level) and Toali cemetery is located in 25 km northwest Khomarlu city with 39° 5' 40" longitude and 46° 49' 5" latitude (330 m above sea level). These cemeteries are located inside Khodafarin and GizGalasi Dams.

Abbreviation codes for these cemeteries are shown in tables including: (1) KH for Khodafarin dam; (2) C for cemetery; (3) LA or TA for Larijan or Toali cemeteries; and (4) K is the cemetery number. For example: KH.C.LA.K4 (Hejabari Noubari, 2007).

The dimensions of these cemeteries are different because people with different social positions were treated differently. Objects that were found in the cemeteries included grey wares, stones, and bronze objects. The cemeteries were used continuously from the late Bronze to Iron I Age.

Ghosha Tepe is located in Ardebil province a distance of 31 km from Meshginshahr in northwest Iran. The Shahryi site is approximate 1.5km from Pierazemeyan village with coordinates of 47° 55' 07" longitude and 38° 33' 53" latitude (1057 m above sea level). The Ghosha tepe site covers an area roughly 80 meters x 114 meters with mounds up to 5 meters tall. This tepe is related to Chalcolithic period. In this tepe 220 pottery sherds (plain and painted) and 1089 stone artifacts were found.

The Khodafarin cemeteries (Hejabari Noubari, 2007) and Ghosha tepe sites were excavated (Hejabari Noubari, 2004) by Alireza Hejabari Noubari of Tarbiat Modares University in Tehran, Iran.

Dem-e-suliman tepe is located about 35 km west of Urmia city next to Moana village. This tepe is at the foot of a mountain area according to surface documentation of ceramics the tepe is related to Neolithic age (Khanmohamady, 2008).

During geological survey, a sample of mother stone (i.e., source sample) with a 10 kg core was found in the east Azerbaijan province of Lilan next to Malkan Township to the SW of Sahand Mountain. A part of this core was removed for analysis. This mother stone is currently in the Tabriz museum. In geology survey, Mansuor Ghorbane of Shahid Beheshti University obtained samples of obsidian from Armenia.

Analytical Methodology

A variety of physical, chemical, and isotopic methods have been employed for obsidian provenance research. However, the three analytical methods most often used today are neutron activation analysis (NAA), X-ray fluorescence (XRF), and laser ablation-inductively coupled plasma-mass spectrometry (LA-ICP-MS). Each of the methods has specific advantages and disadvantages with respect to the analysis of obsidian (Glascock *et al.* 1998). For example, NAA offers excellent sensitivity, precision and accuracy for a large number of elements, and it can be used to analyze the very smallest of samples (e.g., 5 mg). Although NAA is the most reliable and accurate method for most elements, it requires that a portion of the artifact to be destroyed and thereby making the irradiated sample radioactive. NAA is also more expensive and time-consuming than the other analytical methods. XRF offers good sensitivity and accuracy for several of the incompatible trace elements (i.e., Rb, Sr, Y, Zr, and Nb) frequently important for discriminating between obsidian sources (Shackley 1998, 2007). XRF can be performed non-destructively, and it is both a rapid and inexpensive method. However, XRF has limitations when the samples are small, thin, and/or irregularly-shaped. These types of samples may require corrections. Most XRF labs in the world will not attempt to source artifacts smaller than 8mm in diameter and 2 mm thick. The third method of LA-ICP-MS is capable of measuring a large number of elements on very small samples in a relatively short period of time. However, LA-ICP-MS has limitations regarding standardization and instrument stability. XRF was the primary method of choice for this study. To supplement the XRF, some of the samples were also analyzed by NAA.

The obsidian artifacts submitted for analysis ranged in size from less than 5 mm diameter and 1 mm thick up to about 2 cm diameter and 4 mm thick. A majority of the samples were smaller than 1 cm in diameter. Although many of the artifacts were less than ideal, the Archaeometry Lab at MURR has been working on techniques for smaller artifacts (Eerkens *et al.* 2008). Thus far, the techniques have been successfully tested on obsidian from western North America. However, the rate of success for any region is dependent upon the number of possible sources and the similarity of sources to one another. Since the Archaeometry Lab has only recently started to analyze obsidian from the ancient Near East, the sourcing results reported here may have some limitations.

Characterization of Obsidian Sources in the Region

A small number of obsidian from sources in Turkey had been analyzed by the Archaeometry Lab prior to October 2007, but the number of sources in the region is quite large as shown in Figure 1 and the MURR obsidian database for this region was very sparse. As a result, several colleagues were contacted to request the loan of obsidian source materials for compositional analysis at MURR. Jim Blackman (Smithsonian Institution), Bastien Varoutsikos (graduate student from France), Bernard Gratuze (CNRS-France) and Ellery Frahm (graduate student from the University of Minnesota) were extremely helpful in providing a total of 215 obsidian source samples from sources in eastern Turkey, Armenia, Georgia, and Azerbaijan. All of the source samples were analyzed by XRF,

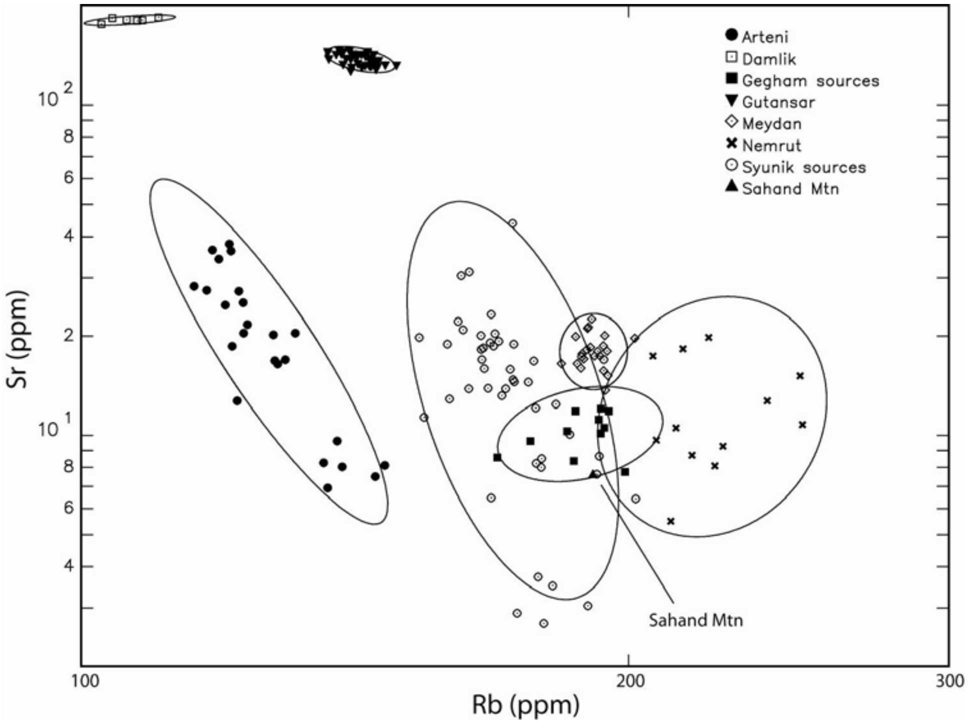

Fig. 2. Log-log bivariate plot of Rb versus Sr measured by XRF for obsidian sources from the ancient Near East relevant to this study. Ellipses at the 90% confidence level surround the source groups.

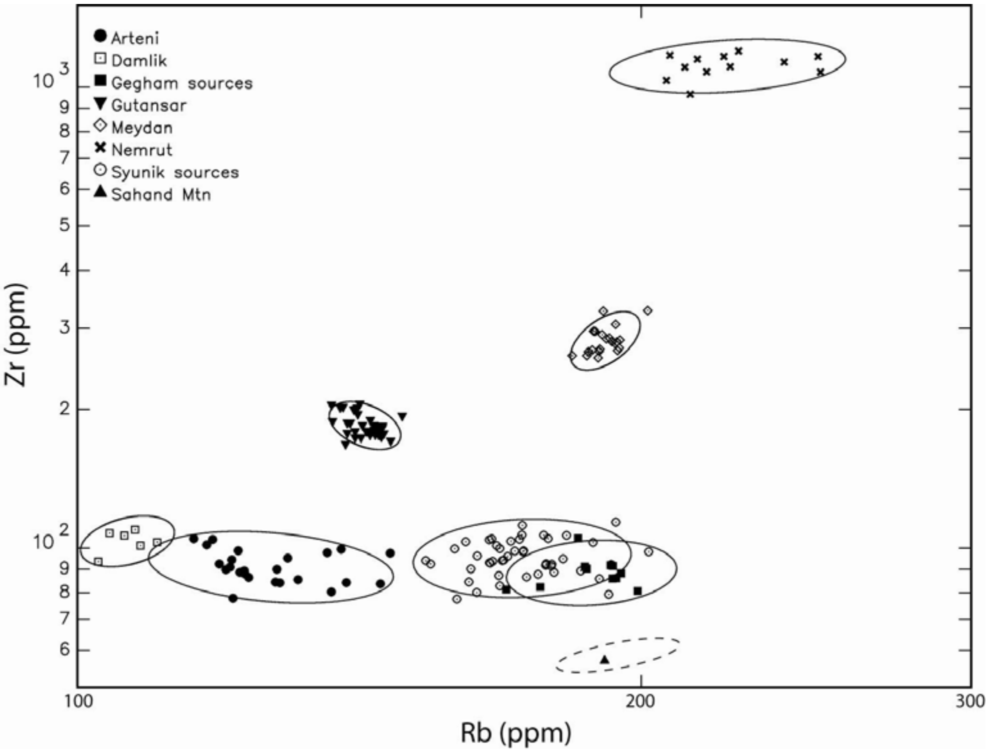

Fig. 3. Log-log bivariate plot of Rb versus Zr measured by XRF for obsidian sources in the ancient Near East relevant to this study. Ellipses at the 90% confidence level surround the source groups.

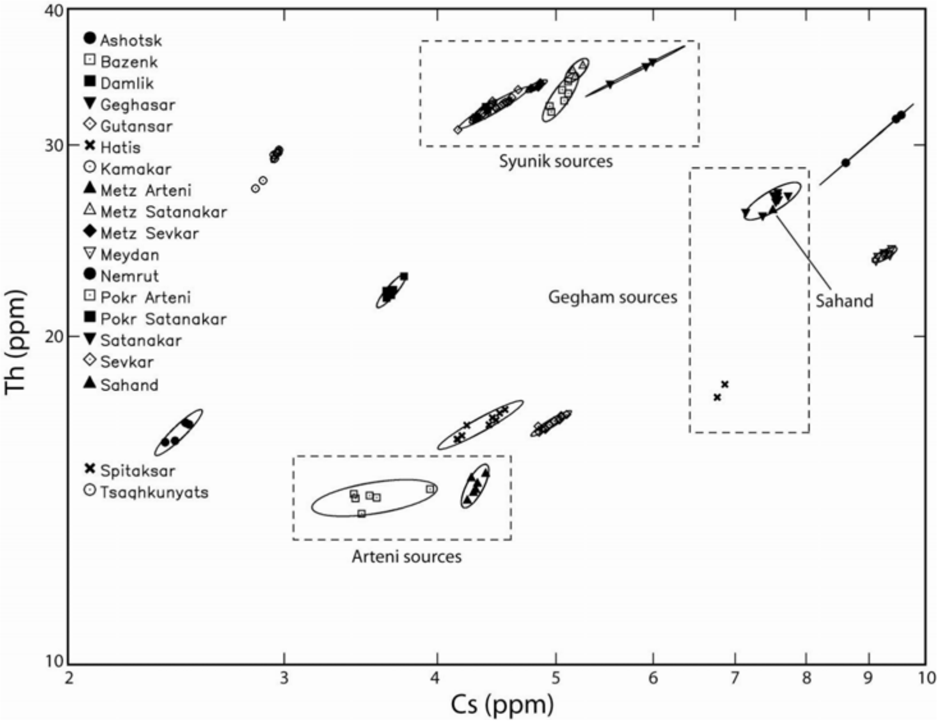

Fig. 4. Log-log bivariate plot of Cs versus Th measured by NAA for obsidian sources in the ancient Near East relevant to this study. Ellipses at the 90% confidence level surround the source groups.

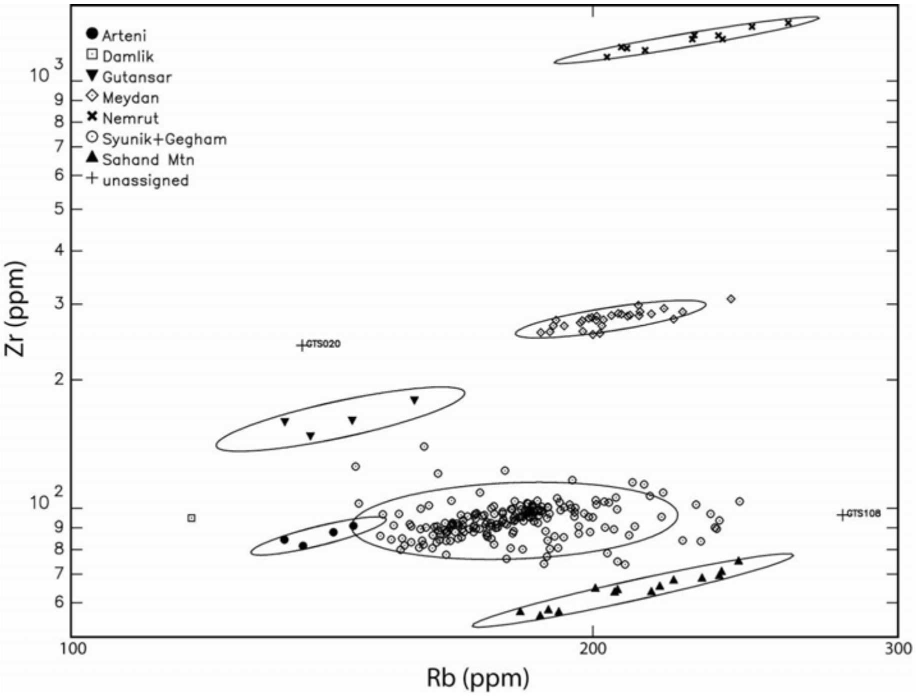

Fig. 5. Log-log bivariate plot of Rb versus Zr measured by XRF for obsidian artifacts from northwestern Iran. Ellipses at the 90% confidence level surround the source groups.

and a smaller subgroup were analyzed by NAA to enhance the Laboratory's ability to differentiate between chemically similar sources.

Examination of the XRF data shows that most, but not all, of the obsidian sources in the region could be differentiated from one another. A few of the neighboring sources in Armenia were found to be chemically similar on most of the measured elements, and a source sample from the Sahand Mountain source was found to be chemically similar to samples from the Geghasar source on many of the elements. These sources were analyzed by both XRF and NAA. The best bivariate plots from the XRF measurements are shown in Figures 2 and 3 where Rb versus Sr and Rb versus Zr, respectively, have been plotted. Figure 4 shows the results possible with NAA when using the high-precision elements Cs and Th.

By XRF, the similarity of source samples lead to the necessity of combining Metz Arteni and Pokr Arteni samples into a single group referred to as the Arteni compositional group; sources at Geghasar and Spitaksar were combined to create the Gegham compositional group; and source samples from Sevkar, Metz Sevkar, Satanakar, Metz Satanakar, Pokr Satanakar, and Bazenk were combined to create the Syunik compositional group. By NAA, it was still very difficult to separate the sources in the Syunik region of Armenia; and the results for the Sahand Mountain sample and samples from the Geghasar source were also found to overlap. In order to differentiate, Sahand Mountain from Geghasar the best available plot is that shown in Figure 3 using the elements Rb and Zr.

Analysis of the Artifacts from Northwestern Iran

All 212 obsidian artifacts and 3 source samples were analyzed by XRF on the Elva-X instrument in the same manner as the source samples. Sample descriptions are listed in Table 1 and the XRF compositional and source assignment data are presented in Table 2. Results for the artifacts analyzed by NAA are listed in Table 3. As shown in Figure 3, the Sahand Mountain sample was found to be unique on a single element with a Zr concentration of about 60 ppm, whereas the most similar source to it is the Geghasar source which has Zr concentrations above 80 ppm. Unfortunately, there was only a single sample from Sahand Mountain available for testing which somewhat limits confidence in assigning artifacts.

Due to the small dimensions for many of the artifacts and the similarity of source compositions it was necessary to combine some of the similar source groups when assigning artifacts from the XRF data. The final XRF results indicated in Table 4 show that 191 artifacts came from the Syunik-Gegham sources, 29 artifacts came from Meydan, 13 artifacts came from Sahand Mountain, 10 artifacts came from Nemrut, 4 artifacts came from Arteni sources, 2 artifacts came from Gutansar, 1 artifact came from Damlik, 11 artifacts were chert, 3 artifacts were basalt, and 2 artifacts could not be assigned. Figure 5 summarizes the obsidian in a plot of Rb versus Zr from XRF data showing these results (without the chert and basalt samples).

Results and Conclusions

With a combination of XRF and NAA measurements on obsidian artifacts from Northwestern Iran, it appears that obsidian trade and exchange between the archaeological sites and sources was quite extensive. Sources in Armenia and Turkey were extremely important and supplied more than 95% of the raw materials found on archaeological sites in northwestern Iran. A single source in Iran at Sahand Mountain provided a small amount of obsidian for local use.

Acknowledgements

We acknowledge the help of James Blackman, Bastien Varoutsikos, Bernard Gratuze and Ellery Frahm for providing source samples from Turkey, Armenia, Georgia, and Azerbaijan and I thank Hossein Esmaeli who is Manager of Tabriz Museum to enable an obsidian source database for the ancient Near East to be established in the Archaeometry Lab at MURR.

References

Eerkens, J.W., J.R. Ferguson, M.D. Glascock, C.E. Skinner and S.A Waechter

2007 Reduction strategies and geochemical characterization of lithic assemblages: A comparison of three case studies from western North America. *American Antiquity* 72(3): 585-597.

Ghorabi, Sohila, Michael D. Glascock, Farhang Khademi, Abdulhamid Rezaie & Mohammad Feizkhah

2008 A geochemical investigation of obsidian artifacts from sites in Northwestern Iran. *International Association of Obsidian Studies Bulletin* 39: 7-10.

Glascock, M.D., G.E. Brawell and R.H. Cobean

1998 A systematic approach to obsidian source characterization. In *Archaeological Obsidian Studies: Method and Theory*, edited by M.S. Shackley, pp. 15-65. Plenum Press, New York and London.

Hejabari, Noubari Alireza

2007 Archaeological Survey and Exploration at the Khodafarin cemeteries. Report to the ICHTO Iranian Center for Archaeological Research in Tehran.

2004 Archaeological Survey and Exploration at the Shahryi of Ardebil. Report to the ICHTO Iranian Center for Archaeological Research in Tehran.

Khanmohamady, Behroz

2008 Archaeological survey at the Urmia township. Report to the ICHTO Iranian Center for Archaeological Research in Urmia.

Shackley, M. Steven

1998 Gamma rays, X-rays and stone tools: Some recent advances in archaeological geochemistry. *Journal of Archaeological Science* 25(3): 259-270.

2008 Archaeological petrology and the archaeometry of lithic materials. *Archaeometry* 50(2):194-215.

KH001	39873	729	302	4467	36	16	157	22	11	92	30	Syunik-Gegham
KH002	42166	831	407	6619	45	18	183	26	13	103	36	Syunik-Gegham
KH003	47889	924	458	5806	53	22	204	20	14	103	42	Syunik-Gegham
KH004	37784	654	319	4208	39	15	168	18	12	91	27	Syunik-Gegham
KH005	38332	583	284	3908	36	15	155	16	11	85	26	Syunik-Gegham
KH006	42334	769	433	5408	40	18	187	18	13	99	34	Syunik-Gegham
KH007	42529	764	389	4820	43	18	181	18	12	95	32	Syunik-Gegham
KH008	40763	721	325	4714	36	17	168	24	12	94	31	Syunik-Gegham
KH009	37760	598	334	4083	33	15	160	17	11	90	27	Syunik-Gegham
KH010	40642	740	364	4981	42	17	186	12	12	92	34	Syunik-Gegham
KH011	38366	610	299	4492	32	15	168	17	11	89	29	Syunik-Gegham
KH012	37416	700	321	4247	45	14	147	14	12	103	27	Syunik-Gegham
KH013	43085	697	387	4981	46	18	198	15	13	97	39	Syunik-Gegham
KH014	44363	710	399	5873	45	19	214	17	15	114	42	Syunik-Gegham
KH015	40546	676	303	4800	41	17	171	23	12	97	32	Syunik-Gegham
KH016	48705	914	510	6017	48	22	220	21	15	109	45	Syunik-Gegham
KH017	40109	639	319	4747	39	16	174	17	11	93	31	Syunik-Gegham
KH018	38992	1430	677	8160	61	18	145	142	19	161	35	Gutansar
KH019	38984	713	293	4300	45	15	151	21	10	86	26	Syunik-Gegham
KH020	59663	973	324	5858	50	30	188	25	13	95	47	Syunik-Gegham
KH021	17385	374	3	925	17	0	15	8	0	3	0	chert
KH022	38502	719	326	4989	34	15	157	23	11	91	32	Syunik-Gegham
KH023	39496	745	296	5163	42	16	171	20	12	88	32	Syunik-Gegham
KH024	35304	648	313	5337	38	13	180	21	12	93	28	Syunik-Gegham
KH025	37185	671	380	4494	35	14	174	15	11	87	32	Syunik-Gegham
KH026	38138	608	266	4124	34	15	159	20	11	84	28	Syunik-Gegham
KH027	42806	859	396	5631	40	19	183	27	12	98	51	Syunik-Gegham
KH028	45292	827	447	5139	46	20	200	17	13	95	35	Syunik-Gegham
KH029	36787	521	397	4953	48	14	196	18	12	91	29	Syunik-Gegham
KH030	39907	640	342	4738	36	16	176	17	12	90	30	Syunik-Gegham
KH031	35798	1466	777	8745	64	17	137	128	18	148	49	Gutansar
GTS001	43914	695	350	4810	42	19	163	14	14	121	32	Syunik-Gegham
GTS002	45338	731	370	5159	46	20	185	19	12	96	40	Syunik-Gegham
GTS003	38211	659	297	4267	34	15	145	13	11	91	27	Arteni
GTS004	38777	600	322	4627	38	15	179	11	11	81	35	Syunik-Gegham
GTS005	41162	732	340	4914	39	17	175	23	13	100	31	Syunik-Gegham

GTS006	41883	673	356	4740	40	17	186	19	13	99	35	Syunik-Gegham
GTS007	42182	584	381	4594	44	18	173	18	12	92	31	Syunik-Gegham
GTS008	40243	696	319	4866	42	16	176	19	12	92	31	Syunik-Gegham
GTS009	38966	677	271	4232	38	15	163	22	12	91	27	Syunik-Gegham
GTS010	43738	670	362	4755	41	19	185	21	13	98	32	Syunik-Gegham
GTS011	43229	670	367	4617	44	18	177	17	13	98	32	Syunik-Gegham
GTS012	43278	748	315	4469	32	19	166	31	11	91	35	Syunik-Gegham
GTS013	38657	696	411	9480	88	16	202	23	40	267	28	Meydan
GTS014	45212	1725	340	27046	277	26	259	24	184	1368	95	Nemrut
GTS015	38747	888	227	20121	186	19	208	21	147	1200	58	Nemrut
GTS016	45058	1333	377	25786	237	24	238	20	162	1252	77	Nemrut
GTS017	40589	654	328	4596	38	17	171	19	11	91	29	Syunik-Gegham
GTS018	41932	645	414	9839	79	18	220	18	46	293	32	Meydan
GTS019	40856	690	410	9211	69	18	200	22	41	279	31	Meydan
GTS020	37931	669	491	7671	68	15	136	5	31	240	25	unassigned
GTS021	40505	695	366	4402	40	16	167	17	12	92	27	Syunik-Gegham
GTS022	42619	755	378	4932	45	18	184	21	13	97	32	Syunik-Gegham
GTS023	44378	749	384	5093	43	19	185	22	13	98	33	Syunik-Gegham
GTS024	45261	836	360	5081	34	20	175	24	13	101	32	Syunik-Gegham
GTS025	45758	824	422	5409	40	20	201	20	14	104	37	Syunik-Gegham
GTS026	49483	916	482	6127	56	23	206	24	14	106	43	Syunik-Gegham
GTS027	41905	676	357	4815	40	18	182	19	13	95	33	Syunik-Gegham
GTS028	51960	886	607	6118	59	25	237	10	14	94	56	Syunik-Gegham
GTS029	41109	690	387	4591	37	17	178	21	12	94	31	Syunik-Gegham
GTS030	62411	986	759	4558	62	32	243	11	18	75	73	Sahand Mtn
GTS031	43377	904	401	5098	44	19	184	25	13	102	35	Syunik-Gegham
GTS032	46362	863	433	5122	47	21	207	16	13	99	45	Syunik-Gegham
GTS033	42171	709	398	5023	42	18	182	19	12	95	35	Syunik-Gegham
GTS034	46885	884	505	4215	48	21	136	36	12	82	34	Arteni
GTS035	50610	895	601	6241	63	24	243	13	15	104	57	Syunik-Gegham
GTS036	39525	655	344	4571	40	16	166	25	12	92	29	Syunik-Gegham
GTS037	44675	769	401	4980	41	19	187	18	13	98	35	Syunik-Gegham
GTS038	41798	620	361	4948	42	17	179	20	13	99	34	Syunik-Gegham
GTS039	44389	770	391	5049	42	19	187	21	13	101	37	Syunik-Gegham
GTS040	45444	618	427	5141	47	20	187	21	13	99	36	Syunik-Gegham
GTS041	41290	679	373	4776	43	17	178	16	12	92	37	Syunik-Gegham

GTS042	42650	705	382	4642	33	18	176	17	11	91	35	Syunik-Gegham
GTS043	43362	558	547	4607	44	18	236	5	13	89	44	Syunik-Gegham
GTS044	38898	539	466	3898	42	15	211	6	12	91	39	Syunik-Gegham
GTS045	52760	1172	338	6024	53	25	188	29	13	101	43	Syunik-Gegham
GTS046	39026	604	377	4257	32	15	180	16	11	87	34	Syunik-Gegham
GTS047	47538	770	456	5134	53	22	188	21	12	88	39	Syunik-Gegham
GTS048	40546	603	368	4182	35	16	188	7	12	84	32	Syunik-Gegham
GTS049	35013	393	347	3317	39	13	187	6	10	74	33	Syunik-Gegham
GTS050	46890	868	487	5901	58	21	195	25	15	116	38	Syunik-Gegham
GTS051	50552	838	343	5005	45	24	185	21	13	102	42	Syunik-Gegham
GTS052	43535	780	390	4825	33	19	185	20	13	98	35	Syunik-Gegham
GTS053	44396	764	447	5207	45	19	185	19	12	93	37	Syunik-Gegham
GTS054	41254	628	683	4853	56	17	231	12	16	69	52	Sahand Mtn
GTS055	46081	848	429	5033	40	20	184	21	13	98	35	Syunik-Gegham
GTS056	43432	736	364	4976	41	19	189	25	13	97	34	Syunik-Gegham
GTS057	43340	674	379	4855	41	18	186	19	12	96	33	Syunik-Gegham
GTS058	46980	776	571	5800	53	21	234	13	14	97	48	Syunik-Gegham
GTS059	44311	673	417	5268	46	19	166	15	13	104	35	Syunik-Gegham
GTS060	51463	1353	718	5785	65	25	154	45	14	91	42	Syunik-Gegham
GTS061	39655	601	331	4024	44	16	178	9	10	76	29	Syunik-Gegham
GTS062	43236	787	403	4821	48	18	177	19	12	93	32	Syunik-Gegham
GTS063	50281	997	514	6115	58	24	216	20	15	107	44	Syunik-Gegham
GTS064	53349	1042	552	5925	54	26	211	20	15	115	47	Syunik-Gegham
GTS065	45366	761	410	5317	46	20	185	24	13	101	36	Syunik-Gegham
GTS066	44120	672	378	4909	40	19	177	24	12	97	33	Syunik-Gegham
GTS067	48321	769	359	4790	34	22	171	24	12	96	35	Syunik-Gegham
GTS068	39890	555	383	4050	35	16	190	8	12	86	33	Syunik-Gegham
GTS069	42805	743	443	5095	41	18	186	17	13	104	31	Syunik-Gegham
GTS070	46525	679	756	4526	51	21	237	10	17	69	59	Sahand Mtn
GTS071	53774	1025	463	5098	49	26	194	20	14	102	43	Syunik-Gegham
GTS072	42161	789	452	5049	41	18	175	24	12	97	34	Syunik-Gegham
GTS073	64096	2091	343	21545	199	37	229	28	162	1281	81	Nemrut
GTS074	45015	753	371	5111	39	20	180	26	13	104	38	Syunik-Gegham
GTS075	60072	1139	425	5194	46	30	184	22	13	98	47	Syunik-Gegham
GTS076	44483	837	420	5230	48	19	172	15	13	109	36	Syunik-Gegham
GTS077	45337	779	392	4476	34	20	176	19	11	90	32	Syunik-Gegham

GTS078	39888	625	367	4349	44	16	167	19	12	91	28	Syunik-Gegham
GTS079	40762	1031	368	22012	191	21	228	27	158	1253	54	Nemrut
GTS080	41838	660	355	4594	40	17	173	23	12	96	33	Syunik-Gegham
GTS081	40062	596	475	4141	35	16	196	9	12	87	31	Syunik-Gegham
GTS082	42047	675	369	4383	42	18	178	17	12	94	30	Syunik-Gegham
GTS083	40242	543	336	4311	36	16	180	14	12	88	32	Syunik-Gegham
GTS084	69542	1333	388	9453	87	38	190	21	40	275	43	Meydan
GTS085	47040	894	418	5622	46	21	199	18	13	95	40	Syunik-Gegham
GTS086	54277	1165	602	6677	62	26	230	16	14	102	49	Syunik-Gegham
GTS087	44736	777	472	5363	53	20	219	11	13	95	43	Syunik-Gegham
GTS088	50247	931	419	5460	44	23	203	22	14	104	43	Syunik-Gegham
GTS089	17256	375	3	5033	23	0	15	6	0	2	0	chert
GTS090	46280	811	434	5397	54	21	195	20	13	100	41	Syunik-Gegham
GTS091	43778	759	404	5071	47	19	188	22	13	100	36	Syunik-Gegham
GTS092	36272	643	309	4846	31	13	163	20	11	87	24	Syunik-Gegham
GTS093	43370	853	410	5743	49	19	178	18	15	122	35	Syunik-Gegham
GTS094	43166	715	339	4953	36	18	180	25	13	99	32	Syunik-Gegham
GTS095	43618	822	382	5338	41	19	192	20	13	99	34	Syunik-Gegham
GTS096	51893	1027	466	5413	52	25	201	20	14	102	46	Syunik-Gegham
GTS097	37641	664	385	6210	42	15	195	20	14	98	32	Syunik-Gegham
GTS098	38005	540	318	4471	28	15	159	21	11	89	29	Syunik-Gegham
GTS099	43112	863	285	5502	36	19	175	46	11	82	31	Syunik-Gegham
GTS100	39398	420	331	4398	39	16	166	18	12	91	29	Syunik-Gegham
GTS101	41683	709	368	4882	45	17	182	20	12	93	37	Syunik-Gegham
GTS102	43735	924	587	4907	49	19	142	26	13	88	30	Arteni
GTS103	52518	773	335	4191	32	25	172	17	12	89	41	Syunik-Gegham
GTS104	37566	634	501	4051	37	15	206	22	14	64	44	Sahand Mtn
GTS105	40898	789	347	5469	34	17	171	29	12	97	30	Syunik-Gegham
GTS106	40431	722	359	5243	45	17	180	21	13	96	36	Syunik-Gegham
GTS107	45901	662	570	4556	48	20	235	5	14	90	41	Syunik-Gegham
GTS108	52829	749	824	6074	67	25	279	6	16	96	65	unassigned
GTS109	44675	670	419	5276	47	20	191	21	13	103	37	Syunik-Gegham
GTS110	39040	684	432	6770	47	16	203	16	13	90	36	Syunik-Gegham
GTS111	41122	578	459	9960	84	18	213	21	44	288	32	Meydan
GTS112	44573	747	404	4922	41	19	182	23	13	99	38	Syunik-Gegham
GTS113	39241	428	474	9344	72	17	210	19	43	283	34	Meydan

GTS114	41635	646	348	4482	43	17	174	14	11	86	34	Syunik-Gegham
GTS115	42709	769	392	4958	48	18	186	19	13	99	32	Syunik-Gegham
GTS116	41289	1259	565	5592	47	19	117	200	11	95	21	Damlik
GTS117	41708	543	444	4643	46	17	206	8	12	89	37	Syunik-Gegham
GTS118	42539	779	419	5133	40	18	161	18	12	102	32	Syunik-Gegham
GTS119	37376	526	570	3087	46	14	189	9	12	58	37	Sahand Mtn
GTS120	39006	618	408	9420	76	17	201	23	41	275	30	Meydan
GTS121	38671	390	467	3890	36	15	204	5	11	78	35	Syunik-Gegham
GTS122	46725	873	404	5380	39	21	182	25	13	101	35	Syunik-Gegham
GTS123	38749	583	408	9332	73	16	197	23	40	271	29	Meydan
GTS124	41353	561	578	3513	34	17	216	8	15	64	48	Sahand Mtn
GTS125	43677	829	289	4793	57	19	170	17	11	89	29	Syunik-Gegham
GTS126	41425	742	312	4493	35	17	169	24	12	96	34	Syunik-Gegham
GTS127	39933	746	280	5045	46	16	164	24	11	92	31	Syunik-Gegham
GTS128	52964	831	353	4442	55	25	165	18	11	88	33	Syunik-Gegham
GTS129	47282	854	442	5564	46	21	191	22	14	106	41	Syunik-Gegham
GTS130	45985	888	353	4888	40	20	180	21	12	95	37	Syunik-Gegham
GTS131	48409	985	460	5146	44	22	192	53	11	85	35	Syunik-Gegham
GTS132	39874	579	381	4129	39	16	189	9	11	80	32	Syunik-Gegham
GTS133	43321	738	378	4615	40	19	183	19	13	99	37	Syunik-Gegham
GTS134	46464	821	475	5532	56	21	184	24	13	101	41	Syunik-Gegham
GTS135	40187	428	340	4696	35	16	174	20	12	91	33	Syunik-Gegham
GTS136	39137	1099	130	21107	206	21	214	40	146	1181	56	Nemrut
GTS137	41674	646	333	4902	40	17	175	19	11	91	31	Syunik-Gegham
GTS138	49842	435	318	4776	40	23	178	23	12	92	37	Syunik-Gegham
GTS139	38709	675	371	5306	53	15	174	20	11	88	32	Syunik-Gegham
GTS140	43531	693	424	4649	41	19	191	12	11	81	27	Syunik-Gegham
GTS141	38214	701	280	4106	34	15	156	18	10	82	30	Syunik-Gegham
GTS142	44983	917	364	4934	44	20	159	20	12	100	40	Syunik-Gegham
UDS001	40489	618	346	9545	72	18	208	19	43	284	32	Meydan
UDS002	44756	1375	172	24847	240	24	247	14	175	1340	83	Nemrut
UDS003	36755	562	277	8712	72	15	199	18	40	277	31	Meydan
UDS004	42665	1183	162	23572	227	22	236	14	164	1277	72	Nemrut
UDS005	43507	882	109	7395	33	19	160	24	20	139	21	Syunik-Gegham
UDS006	41626	702	388	10304	91	19	216	19	44	284	38	Meydan
UDS007	38016	677	305	4469	36	15	175	17	12	92	29	Syunik-Gegham

UDS008	38043	554	350	9739	72	16	209	18	43	281	28	Meydan
UDS009	40541	658	340	10313	74	18	213	20	45	298	29	Meydan
UDS010	38588	562	376	9591	74	16	207	18	43	285	30	Meydan
UDS011	40172	631	334	4674	40	16	168	23	12	96	31	Syunik-Gegham
UDS012	37540	609	265	9369	67	15	203	17	41	275	31	Meydan
UDS013	43331	798	349	4883	43	19	184	18	13	96	37	Syunik-Gegham
UDS014	47028	660	712	4607	48	21	237	9	17	71	58	Sahand Mtn
UDS015	44356	730	475	11648	91	21	240	19	51	308	38	Meydan
UDS016	40506	685	293	8878	67	17	189	18	38	258	30	Meydan
UDS017	42718	704	335	4887	38	18	184	19	12	95	32	Syunik-Gegham
UDS018	47967	618	575	3373	39	22	207	8	14	64	51	Sahand Mtn
UDS019	41893	621	675	4373	48	18	223	10	16	68	50	Sahand Mtn
UDS020	34564	495	439	3316	35	12	182	8	12	57	34	Sahand Mtn
UDS021	40310	420	605	3680	43	16	219	9	15	66	49	Sahand Mtn
UDS022	45328	765	334	4748	35	20	173	18	12	96	37	Syunik-Gegham
UDS023	43360	843	353	5360	42	19	194	20	13	100	35	Syunik-Gegham
UDS024	42886	723	391	5061	44	18	193	19	13	100	37	Syunik-Gegham
UDS025	43665	880	497	4384	40	19	133	39	12	84	32	Arteni
UDS026	43617	798	329	5091	52	19	180	25	13	100	35	Syunik-Gegham
UDS027	36977	613	396	9215	77	15	197	22	39	259	33	Meydan
UDS028	40320	447	445	11485	87	18	223	24	43	277	41	Meydan
UDS029	38178	1059	114	20061	176	20	204	43	137	1138	57	Nemrut
UDS030	45854	832	494	11970	97	22	225	24	46	288	40	Meydan
UDS031	42108	663	155	6852	32	18	146	24	17	125	18	Syunik-Gegham
UDS032	41267	676	302	10460	80	18	213	24	43	282	38	Meydan
UDS033	38539	685	346	4240	32	15	166	17	11	84	25	Syunik-Gegham
UDS034	33941	577	361	10121	78	13	202	27	38	256	26	Meydan
UDS035	31658	408	509	3238	39	10	187	8	11	56	38	Sahand Mtn
UDS036	42317	734	393	4676	31	18	171	22	12	95	31	Syunik-Gegham
ARM001	36476	1219	605	7481	53	17	133	140	19	160	33	Gutansar
ARM002	40063	1633	665	8896	47	20	158	151	22	179	38	Gutansar
Sahand	36484	406	533	3049	26	14	191	8	12	57	39	Sahand Mtn

BODIE HILLS OBSIDIAN FROM MONO COUNTY, EASTERN CALIFORNIA: A HYDRATION RATE AND AN ISSUE

Alexander K. Rogers, MA, MS
Archaeology Curator and Staff Archaeologist
Maturango Museum

Abstract

This paper reports a hydration rate for Bodie Hills obsidian from Mono County in Eastern California USA, based on obsidian – radiocarbon pairing data from the western slope of the Sierra Nevada. The analysis employs regional temperature scaling to determine site temperature parameters, and temperature-dependent hydration theory to compute hydration rim corrections for effective hydration temperature (EHT), including the effects of paleoclimatic change and artifact burial depth. The rate is based on a linear least-squares best fit employing the Total Least Squares algorithm, which takes into account uncertainties in both variables and employs both error-based and judgmental weighting. The resulting hydration age coefficient is 103 ± 25 radiocarbon yrs/μ^2, which is reasonably consistent with prior studies. However, this result is not consistent with rates developed for the eastern slope of the Sierra Nevada when temperature differences are taken into account. This discrepancy cannot be resolved until better data on the chemistry, chemical variability, and rate variability of Bodie Hills obsidian are available.

Introduction

This paper proposes a tentative hydration rate for Bodie Hills obsidian, whose source is in Mono County in eastern California, USA. The calculations are based on obsidian-radiocarbon pairing data from the western slope of the Sierra Nevada, kindly provided by Jay Rosenthal of Far Western Anthropological Research Group. The calculation explicitly takes effective hydration temperature (EHT) into account in computing the rate, using temperature parameters computed from 30-year weather data by regional temperature scaling (Rogers 2007b). All EHT values are corrected for burial depth of the artifact. The output is a hydration age coefficient (reciprocal of the rate) applicable to the western slope of the Sierra Nevada. The tentative nature of this rate must be emphasized. The data set employed is relatively error-prone, and an attitude of skepticism is appropriate in applying the rate in chronological analyses, especially since the age coefficient is not consistent with the value for the eastern slope.

I recognize the viewpoint of those who argue that laboratory hydration techniques are the best way to measure rates (e.g. Stevenson et al. 1998). However, most practical rate determinations are still based on obsidian – radiocarbon pairing, and this paper is a modest attempt to optimize this technique by advanced numerical analysis.

Obsidian Hydration

Hydration of obsidian has both a physical and a chemical aspect, and is known as a diffusion-reaction process (Doremus 1994, 2000, 2002). The process is described by a second order partial differential equation, which predicts the concentration of diffusing molecules (i.e. water) as a function of time and depth within the obsidian (Crank 1975:4, eq. 1.6; Doremus 2002:9ff.). The equation has a closed-form solution in only a few cases; however, all these solutions have the property that the concentration of diffusing molecules can be written as a function of a single parameter, $z = \sqrt{(r^2/Dt)}$, where r is rim depth, t is time, and D is the diffusion coefficient. This equation also holds if D is a function of time, in which case D is replaced by its time average (Crank 1975:104-105). Although the equation was first derived for the case of D being constant in x and t (Crank 1975:4ff), it also holds if D is a function of concentration (Crank 1975:119-121; Rogers 2007a; Wagner:1950), which seems to be the case in hydration (Anovitz et al. 1999; Doremus 2002).

The rim thickness is defined physically by the optical hydration front, which is a region of mechanical stress between the hydrated and unhydrated volumes of the glass, and is defined mathematically by a specific point on the concentration-vs.-depth curve for the diffusing water. The point is often assumed for convenience to be the 50% point on the curve, but is more likely to be the inflection point, since that is the point of maximum mechanical stress (Rogers 2008a); the two points are close enough together that the difference is not significant experimentally, although it can be observed by SIMS (Stevenson et al. 2004). The point on the concentration curve defining the rim thickness thus progresses by the equation

$$r^2 = Dt. \qquad (1)$$

All that is known of the physics and chemistry of the process suggests the validity of equation 1, and no other form of functional dependence is currently suggested by theory (see e.g. Doremus 2000, 2002; Ebert et al. 1991; Stevenson et al. 1989, 1998; Zhang et al. 1991). In fact, Haller argued, based on the physical chemistry of diffusion, that if any dependence other than quadratic is found, "it is more likely the fault of the experiment rather than any inherent feature of the diffusion process" (Haller 1963:217). Use of another mathematical form, such as a power law or a polynomial, may give a better fit to a particular data set (as is the case here), but has no foundation in diffusion mechanics. Furthermore, the accuracy of an alternative fit is spurious, since it is simply fitting the experimental errors in the data set, and there is no guarantee that any new data points will fit. The analysis here uses the quadratic form only.

For the case of obsidian, the "hydration rate" is equivalent to the diffusion coefficient D in equation 1. Also, the hydration rate varies with EHT (e.g. Hull 2001; Onken 2006; Ridings 1996; Rogers 2007a; Stevenson et al. 1989, 1998, 2004), with relative humidity (Friedman et al. 1994; Mazer et al. 1991; Onken 2006; Rogers 2008a), and with structural water concentration in the obsidian (Ambrose and Stevenson 2004; Friedman et al. 1966; Rogers 2008c; Stevenson et al. 1998, 2000). The analysis below explicitly treats EHT, while humidity effects are typically small and are ignored. Structural water concentration has never been measured for Bodie Hills obsidian; however, since it is a "slow" obsidian, it is likely that structural water concentration is very low. Its chemical variability has not been characterized.

The analysis here controls for EHT by the temperature-dependent diffusion technique (Rogers 2007a, 2008c), which explicitly accounts for average annual temperature, mean annual temperature variation, mean diurnal temperature variation, and burial depth. It has been further shown that, although EHT exhibits a small dependence on the activation energy of the obsidian, the effect is second-order and can be ignored in practical analyses (Rogers 2007a).

The equation for EHT is

$$EHT = T_a\times(1-Y\times3.8\times10^{-5}) + 0.0096\times Y^{0.95} \quad (2)$$

where T_a is annual average temperature, and the variation factor Y for surface artifacts is defined by

$$Y = V_a^2 + V_d^2\,, \qquad (3a)$$

in which V_a is annual temperature variation (July mean minus January mean) and V_d is mean diurnal temperature variation (Rogers 2007a).

For buried artifacts, V_a and V_d represent the temperature variations at the artifact burial depth, which are related to surface conditions by

$$V_a = V_{a0}\exp(-K_a z) \qquad (3b)$$

and

$$V_d = V_{d0}\exp(-K_d z) \qquad (3c)$$

where V_{a0} and V_{d0} represent nominal surface conditions and z is burial depth (Carslaw and

Jaeger 1959:81). Here K_a and K_d are the attenuation coefficients for the annual and diurnal temperature variations, respectively; they are related to the thermal diffusivity of the soil by the equation

$$K_{a,d} = (\pi/dP_{a,d})^{1/2} \qquad (4)$$

where d is thermal diffusivity and $P_{a,d}$ is the period of the annual or diurnal temperature variation (1 day for diurnal, 365.25 days for annual). The value of d varies between 0.0046 cm^2/sec for normal soil and 0.0020 cm^2/sec for dry sand (Carslaw and Jaeger 1959; App. 4). For this analysis a mean value of 0.0033 cm^2/sec was used. This dependence of temperature variation on depth is well attested in physics, geology, and soil science.

Once EHT has been computed, the measured rim thickness is multiplied by a rim correction factor (RCF) to adjust the rims to be comparable to conditions at a reference site:

$$RCF = \exp[-0.06(EHT-EHT_r)] \qquad (5)$$

where EHT_r is effective hydration temperature at the reference site. The EHT-corrected rim value r_c is then

$$r_c = RCF \times r \qquad (6)$$

The rim value r_c is used in the rate analysis.

Temperature Scaling

Computation of EHT by the method above requires three temperature parameters for the site, as shown in equations 2 and 3a: annual average temperature (T_a); annual temperature variation (V_a), defined as difference between the July average temperature and the January average temperature; and mean diurnal variation (V_d), defined as the average of the daily temperature ranges for July and January. In meteorological terms, V_a is the annual range and V_d is mean diurnal range.

Frequently there are no long-term meteorological records for the area of an archaeological site, so the parameters must either be scaled from a surrogate site or measured. Regional scaling is the method employed here (Rogers 2007b), which ensures that the parameters are computed from a sufficiently long run of data to be representative of long-term climate. Sensors emplaced at a site do not provide this, so all of the computations discussed here are based on data covering a period of 30 years, in accordance with standard meteorological practice (Cole 1970).

The analysis which developed the scaling equations was based on monthly temperature data from the Western Regional Climate Center (WRCC), using the data base from 1971 – 2000. Since the obsidian-radiocarbon pairing data are from the western slope of the Sierra Nevada, the temperature analysis drew from sites in the same region. Eleven sites are represented, varying in altitude from sea level to 3700 feet above mean sea level (amsl), and in similar weather patterns. Details of the analysis may be found in Rogers 2008b.

The analysis showed the effects of a complicating factor not present east of the Sierra Nevada: the Central Valley temperature inversion layer at about 1500 feet, a well-known meteorological phenomenon. Below this altitude, all three temperature parameters are essentially independent of altitude, while above it they scale with altitude.

Annual average temperature, T_a, has an average value of 15.85°C below 1500 ft. Above 1500 ft the value of T_a is given by

$$T_a = 19.44 - .0027x, \quad 1500 < x < 4000 \quad (7)$$

where x is altitude in feet. The 1-sigma accuracy is 0.42°C below 1500 feet and 0.14°C at higher altitudes.

Annual variation, V_a, again exhibited a break at about 1500 ft. The average value of V_a below 1500 ft is 16.02°C, while above 1500 ft the value is

$$Va = 20.75 - .0029x, \quad 1500 < x < 4000 \quad (8)$$

The 1-sigma accuracy of this fit is 0.34° below 1500 feet and 0.23°C above.

The scaling for diurnal variation, V_d, shows a poorer correlation with altitude. Since V_d represents a difference of measured quantities, the instability is not unexpected. In addition, the data represent short-term phenomena and microclimates, which tend to be less stable than long-term parameters. For sites below 1500 ft, the best fit is the mean value of V_d of 14.77°C; above that altitude, the best fit is

$$V_d = 18.57 - .0015x, \qquad 1500 < x < 4000 \qquad (9)$$

One sigma accuracy is 1.67°C below 1500 feet and 0.95°C above that level.

Finally, equations 7 – 9 can be combined with equations 2 and 3 to yield an approximate relationship between EHT and site altitude for the western slope of the Sierra Nevada. The equation is

$$EHT = 18.91°C, \quad 0 \le x \le 1500 \text{ feet} \qquad (10a)$$

$$EHT = 23.89 - 0.0034x, \quad 1500 < x < 4000 \text{ feet.} \qquad (10b)$$

When EHT is computed from equation 2 using parameters of the stated accuracies, the overall accuracy of EHT is 0.40°C below 1500 feet and 0.06°C at higher altitudes.

Data Sets

Three data sets are used in this analysis: radiocarbon data, obsidian data, and site temperature data. Obsidian-radiocarbon pairs used in this analysis are summarized in Table 1; all are from the western slope of the Sierra Nevada.

The first data set is the radiocarbon data, shown in Table 1. The time parameter in equation 1 must be measured from the date the rim was measured, which is closer to 2000 than to the 1950 "present" in the radiocarbon terms. Thus, in performing the analysis, 50 years was added to the radiocarbon age; the age equation must subsequently subtract 50 years to be in rcybp. Ideally the time should be in actual calendar, or clock, time, not radiocarbon years; However, an analysis showed that converting ages to calendar years did not improve the fit (probably due to the poor quality of the data), so the analysis was carried out in radiocarbon years.

The second data set is the obsidian data, also shown in Table 1. Since the hydration rims are expected to conform to a model of the form of equation 1, they should be approximately linear in a plot of rim-squared (r^2) vs. time (t). Figure 1 shows that the basic fit is rather poor. Not only is there scatter in the data, but the rim values are systematically too high for ages below 2500 rcy, and too low for ages above 2500 rcy.

The source of these errors could be one or more of three factors: laboratory errors in rim measurement, errors due to rate variations caused by chemical (especially intrinsic water) variations in the obsidian, or obsidian-radiocarbon association errors due to site formation processes. Rim measurement errors reported by laboratories are typically of the order of 0.01 - 0.05μ, and may be expected to be consistent from one sample to the next. Figure 2 shows the observed error standard deviations for those samples with sample size $N > 1$; it is clear that the errors are not consistent, and exceed the expected magnitude for laboratory errors. Further, it can be shown that the coefficient of variation (CV) for errors arising from rate variations should be independent of the age of the sample; Figure 3 shows this not to be the case. It is therefore likely that the errors are arising in the obsidian-radiocarbon association process due primarily to site formation processes, although the presence of multiple obsidian subsources in the data set, with slightly different hydration rates, cannot be entirely ruled out.

The third data set is comprised of the temperature parameters for the archaeological sites of Table 1. These parameters were computed from the site elevation data by equations 7 – 9, and are summarized in Table 2. Figure 4 shows the resulting surface EHT values.

Seq. No.	Site	Context	Elevation meters amsl	^{14}C BP	+/-	median intercept (cal BP)	Mean (μ)	Bodie Hills Rim Values (μ)						
1	CAL-991	Component 991A1, 0-20 cm	1005	250	60	300	1.3[1]	1.2	1.2	1.3	1.4	1.4		
2	TUO-2197	Unit 4/5, Feature 3, 30-35 cm	870	270	70	330	2.2	1.5	2.0	2.2	2.3	2.3	2.4	2.6
3	Same as #2		870	270	50	340								
4	TUO-407	Unit N104/E97: Feat 6 fill, 20 cm	610	320	110	363	1.9	1.8	1.9					
5	CAL-114/H	Unit 7; Feature 2, 38-73 cm	1050	360	70	400	1.9[2]	1.3	1.6	1.7	1.7	1.8	2.4	3.1
6	AMA-56	Feature 1B: 60-76 cm	65	1160	60	1080	3.1	-						
7	CAL-789	Unit S44/W30: 20-50 cm	450	1220	40	1160	3.6	3.3	3.6	3.6	3.7			
8	CAL-789	Unit S10/E20: 30-40 cm	450	1270	40	1210	3.4	-						
9	PLA-695/H	Unit 95Q: 130-140 cm	670	1340	60	1255	3.8	3.5	3.8	4.0				
10	SAC-60	Burial 38-11, 122 cm	2	1550	150	1465	4.0	3.8	4.1					
11	PLA-695/H	Unit 95F: 70-90 cm	670	2170	70	2175	4.5	-						
12	SJO-142	Burial 18, 71 cm	0	2495	120	2560	4.8	-						
13	CAL-789	Feature 1, 60-80 cm	450	2510	40	2580	3.9	-						
14	SJO-68	Burial 23, 120 cm	0	3775	160	4155	4.9	4.8	4.9					
15	SJO-68	Cremation 1, 119 cm	0	4350	250	4950	5.5	-						
16	CAL-629/630	90N/26E, Feat. 232, Black Clay: 203-212 cm	305	8510	150	9050	7.3[3]	6.5	6.9	7.0	7.4	7.4	7.4	
17	Same as # 16			8630	145	9370								
18	CAL-629/630	96N/25E, Green Clay, : 225-235 cm	305	9040	90	9990	7.3	6.4	6.6	6.8	7.4	7.5	7.5	
								7.7	7.7	7.7	7.8			
19	CAL-629/630	93N/24E, Feat 212, Black Clay: 170-200 cm	305	9230	100	10195	7.4	-						
20	CAL-629/630	86N/23E, Black Clay: 190-200 cm	305	9240	150	10200	8.2	-						

[1] excludes outlier of 3.0; [2] excludes outlier of 4.4μ; [3] excludes one outlier of 10.4μ; outliers removed using Chauvenet's Criterion

Table 1. Obsidian-radiocarbon pair data from western Sierran slope sites. From Rosenthal and Waechter (2002).

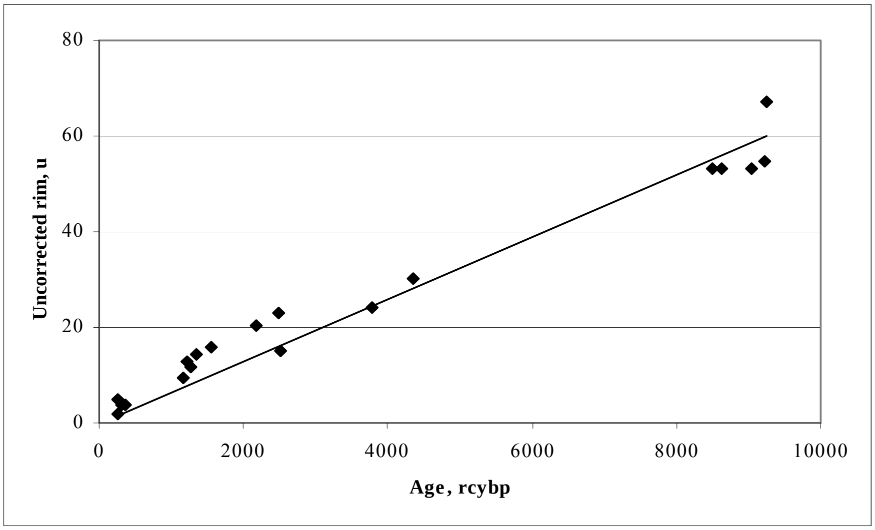

Fig. 1. Uncorrected rim data from the western Sierran slope.

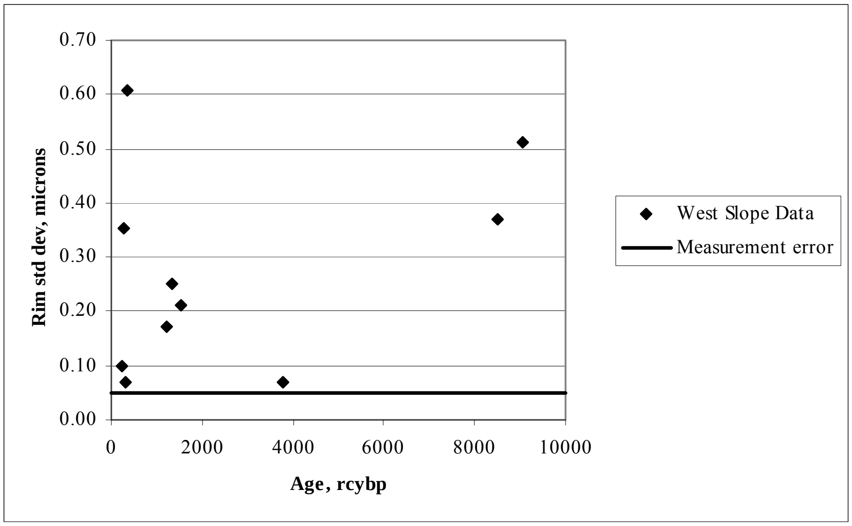

Fig. 2. Sample standard deviation for hydration rims from western Sierran slope sites. Only samples with N>1 are included.

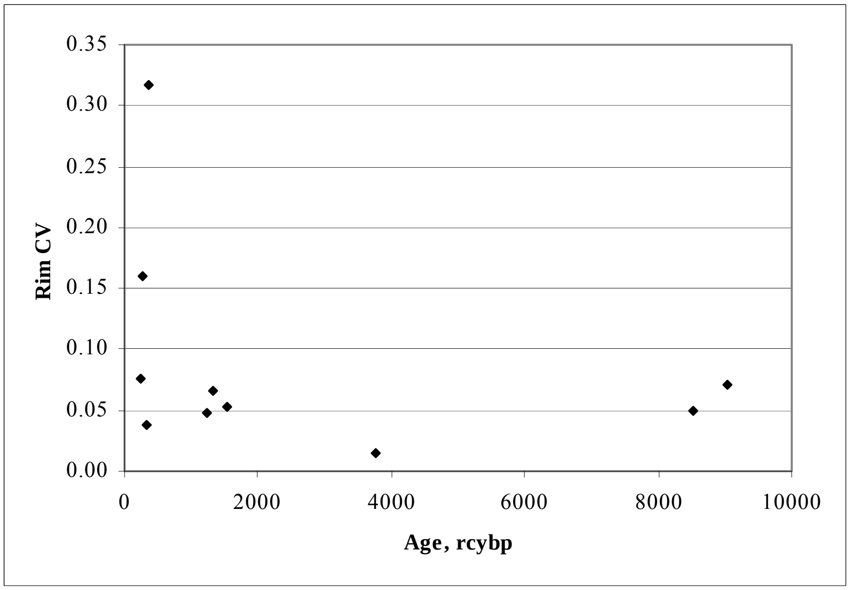

Fig. 3. Coefficient of variation (CV) for hydration rims from western Sierran slope sites. If they were due to rate variability, such as from obsidian chemistry variations, the values would be approximately equal.

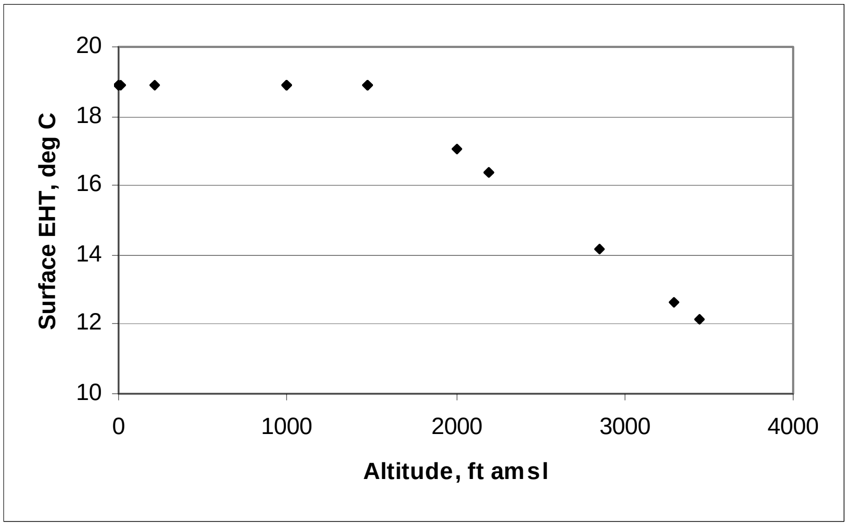

Fig. 4. Surface EHT data for western Sierran slope sites. In performing the age coefficient analysis, EHT is corrected for depth for buried artifacts.

Seq. No.	Site	Context	Elevation meters amsl	Elevation kft amsl	Ta	Va	Vd	Y	EHTz
1	CAL-991	Component 991A1, 0-20 cm	1005	3296	10.54	11.19	13.63	310.79	12.65
2,3	TUO-2197	Unit 4/5, Feature 3, 30-35 cm	870	2854	11.74	12.47	14.29	359.71	14.15
4	TUO-407	Unit N401/E97: Feat 6 fill, 20 cm	610	2001	14.04	14.94	15.57	465.70	17.08
5	CAL-114/H	Unit 7; Feature 2, 38-73 cm	1050	3444	10.14	10.76	13.40	295.41	12.16
6	AMA-56	Feature 1B: 60-76 cm	65	213	15.85	16.02	14.77	474.79	18.91
7	CAL-789	Unit S44/W30: 20-50 cm	450	1476	15.85	16.02	14.77	474.79	18.91
8	CAL-789	Unit S10/E20: 30-40 cm	450	1476	15.85	16.02	14.77	474.79	18.91
9	PLA-695/H	Unit 95Q: 130-140 cm	670	2198	13.51	14.37	15.27	439.86	16.40
10	SAC-60	Burial 38-11, 122 cm	2	7	15.85	16.02	14.77	474.79	18.91
11	PLA-695/H	Unit 95F: 70-90 cm	670	2198	13.51	14.37	15.27	439.86	16.40
12	SJO-142	Burial 18, 71 cm	0	0	15.85	16.02	14.77	474.79	18.91
13	CAL-789	Feature 1, 60-80 cm	450	1476	15.45	16.47	16.36	538.63	18.91
14	SJO-68	Burial 23, 120 cm	0	0	15.85	16.02	14.77	474.79	18.91
15	SJO-68	Cremation 1, 119 cm	0	0	15.85	16.02	14.77	474.79	18.91
16,17	CAL-629/630	90N/26E, Feat. 232, Black Clay: 203-212 cm	305	1000	15.85	16.02	14.77	474.79	18.91
18	CAL-629/630	96N/25E, Green Clay, : 225-235 cm	305	1000	15.85	16.02	14.77	474.79	18.91
19	CAL-629/630	93N/24E, Feat 212, Black Clay: 170-200 cm	305	1000	15.85	16.02	14.77	474.79	18.91
20	CAL-629/630	86N/23E, Black Clay: 190-200 cm	305	1000	15.85	16.02	14.77	474.79	18.91

Table 2. Temperature data for western Sierra slope sites, based on temperature scaling derived from 30-year meteorological records.

Analytical Process

Since equation 1 is quadratic, the analysis process is to compute a linear least-squares best fit between r^2 and t, with the resulting slope being the rate. A simple form of the best fit slope for an equation constrained to pass through the origin can be found in many references (e.g. Meyer 1975:71ff., Cvetanovic et al. 1979). However, a critical assumption in using such an equation is that the independent variable be error-free, and all error be confined to the dependent variable. This is clearly not the case for obsidian, since significant experimental error exists in both variables; in fact, for the present data set the error CVs for both t and r^2 are of the order of 30%, so use of the simple fit equations is inappropriate for this case. (This includes the built-in SLOPE and INTERCEPT functions in MS Excel – use of these functions can lead to incorrect answers.)

The error-in-both-variables problem can be avoided by using a best-fit algorithm which weights the data points by the sum-squared deviation from the best fit line, *measured perpendicular to the line* (Meyer 1975; called the Total Least Squares – TLS - algorithm by Van Huffel and Vandewalle 1991). This is the algorithm applied here.

Any least-squares best fit algorithm includes provision for weighting of individual data points, such that more confidence is placed on high-quality data points and less on lower-quality data (Cvetanovic et al. 1979). The TLS algorithm, as developed here, applies two types of weighting to the variables: error weighting, or weighting by the inverse of the error variance characteristic each data point; and judgmental weighting, a factor which assigns higher confidence to certain data points; the details of this procedure are discussed below.

For this analysis, age, t, is chosen as the independent variable, in accordance with the physical process, and the square of the hydration rim, r^2, is the dependent variable; change of variable weighting is applied to optimize errors in r (Cvetanovic et al. 1979). With change of variable, the TLS algorithm for the slope (or hydration rate) is

$$m = [-B + \sqrt{(B^2 + 4AC)}]/2A \qquad (11a)$$

where

$$A = \sum w_i t_i r^2_i (\sigma_{ti})^2 / \sigma_{mi}^4 \qquad (11b)$$

$$B = \sum w_i [t_i^2 (\sigma_{ri})^2 - r_i^4 (\sigma_{ti})^2] / \sigma_{mi}^4 \qquad (11c)$$

$$C = \sum 4 w_i t_i r^4_i (\sigma_{ri})^2 / \sigma_{mi}^4 \qquad (11d)$$

$$\sigma_{mi}^2 = 4r^2 (\sigma_{ri})^2 + m^2 (\sigma_{ti})^2 \qquad (11e)$$

Here t_i is the age of the i^{th} point, r_i is the EHT-corrected rim value, w_i is the judgmental weight, $(\sigma_{ti})^2$ is expected error variance of the i^{th} data point in the t dimension, $(\sigma_{ri})^2$ is the corresponding error variance in the r dimension, and σ_{mi}^2 is the error variance perpendicular to the best-fit line. Note that $(\sigma_{ti})^2$ and $(\sigma_{ri})^2$ refer to error statistics, not the instantaneous deviation of each point from the best-fit line. The implementation of this algorithm is iterative, because the unknown (m) occurs on both sides of equations 11.

For the first step, corrections for EHT were computed for each hydration rim value in Table 1. This entailed drawing the temperature parameters for each site from Table 2, and applying depth corrections per equations 3b and 3c. Using the depth-corrected parameters, EHT was then computed by equations 2 and 3, and the rim correction factor computed from equations 5 and 6. A reference EHT of 18.91°C was chosen, characteristic of the Central Valley below 1500 ft altitude.

Judgmental weights were chosen based on examination of the data of Table 1 and the plot in Figure 1. The baseline chosen was $w_i = 1$ for all data points. However, a greater weight ($w_i = 2$) was assigned to the four data points which derived from burial contexts; this was because association in burials is usually better than in non-burial contexts, and also because burials tend to be excavated more carefully. Finally, a lesser weight ($w_i = 0.5$) was assigned to the data points from CAL-629/630, due to the very large scatter in the data evident in Figure 1.

The values of $(\sigma_{ti})^2$ and $(\sigma_{ri})^2$ were developed iteratively by computing an initial best fit, observing data points for logical groupings, computing the variances for these groupings, and recomputing the best fit using the new variances. The process was repeated until the value of the age coefficient converged to a stable value, typically after four or five iterations.

This process led to computation of the age coefficient h, the reciprocal of rate, which permits convenient computation of age by equation 12:

$$t = hx^2 \quad - 50 \qquad (12)$$

The results for an EHT of 18.91°C are:

$$t_{rcybp} = 103.09r^2 - 50, \text{ for } 0 \leq r \leq 8\mu. \qquad (13)$$

Potential errors in the age coefficient are, however, significant. If the same analysis is run with the data set excluding CAL-629/630, the age coefficient h is approximately 10% smaller than in equations 12 and 13; if the analysis is run on CAL-629/630 data alone the value of h is about 10% greater. Computing the slope based on burials alone results in an h value about 5% smaller. This confirms the marginal quality of the data set, because excluding parts of a data set should not lead to such large changes; there is no way to resolve these error sources once the input data are specified (Gerald and Wheatley 1984; Johnson and Riess 1982).

Although derived by the best numerical analysis techniques available, these age coefficients do not yield a particularly good fit archaeologically. In Table 3 the computed ages in rcybp are compared to the radiocarbon ages; the errors are summarized in Figure 5. Mean error is 107 years, which is reasonably good, but standard deviation is 796 years, which is not. Examination of Figure 6 shows there is also a systematic error present, with ages below 2500 rcybp consistently underestimated and ages over that age overestimated. Use of a power law with exponent greater that 2 will yield a closer fit; however, it represents a fit to the effects of site formation processes, and there is no reason to expect it to be significant. The error standard deviation of 796 yrs corresponds to an overall error margin in hydration age coefficient of about ±25%.

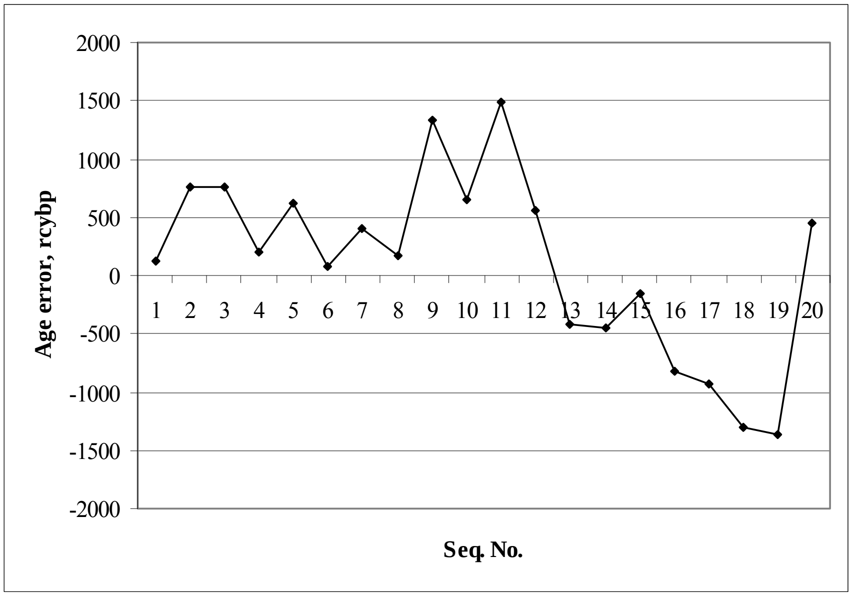

Fig. 5. Estimation error in age. Error standard deviation is 796 years.

Seq. No.	Site	Context	RC age, rcybp	Est age, rcybp	Error, rcy
1	CAL-991	Component 991A1, 0-20 cm	250	381	131
2	TUO-2197	Unit 4/5, Feature 3, 30-35 cm	270	1025	755
3	TUO-2197	Same as #2	270	1025	755
4	TUO-407	Unit N401/E97: Feat 6 fill, 20 cm	320	524	204
5	CAL-114/H	Unit 7; Feature 2, 38-73 cm	360	979	619
6	AMA-56	Feature 1B: 60-76 cm	1160	1242	82
7	CAL-789	Unit S44/W30: 20-50 cm	1220	1622	402
8	CAL-789	Unit S10/E20: 30-40 cm	1270	1441	171
9	PLA-695/H	Unit 95Q: 130-140 cm	1340	2681	1341
10	SAC-60	Burial 38-11, 122 cm	1550	2197	647
11	PLA-695/H	Unit 95F: 70-90 cm	2170	3658	1488
12	SJO-142	Burial 18, 71 cm	2495	3058	563
13	CAL-789	Feature 1, 60-80 cm	2510	2087	-423
14	SJO-68	Burial 23, 120 cm	3775	3318	-457
15	SJO-68	Cremation 1, 119 cm	4350	4191	-159
16	CAL-629/630	90N/26E, Feat. 232, Black Clay: 203-212 cm	8510	7695	-815
17	CAL-629/630	Same as #16.	8630	7695	-935
18	CAL-629/630	96N/25E, Green Clay, : 225-235 cm	9040	7733	-1307
19	CAL-629/630	93N/24E, Feat 212, Black Clay: 170-200 cm	9230	7859	-1371
20	CAL-629/630	86N/23E, Black Clay: 190-200 cm	9240	9690	450

Table 3. Estimation errors from equations 12-13.

These values apply only to the reference temperature of 18.91°C, and the value of h is very sensitive to EHT (which is why references to rates for “eastern slope” or “western slope” are overly simplistic and should be avoided). In fact the value of h varies with EHT by the equation

$$h_s = h_r \times \exp[-.12(EHT_s - EHT_r)] \quad (14)$$

where h_s is the value of h at a site being analyzed, EHT_s is the surface EHT at that site, and h_r is the value of h at the reference EHTr. Combining the

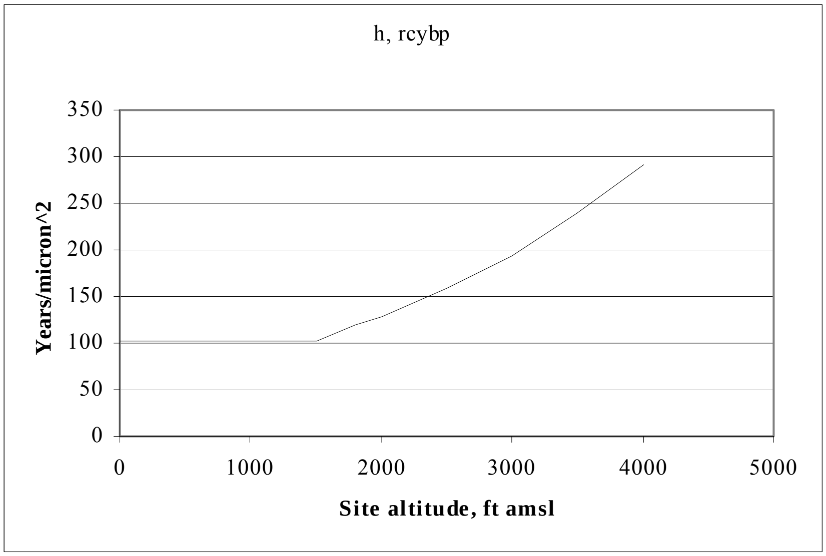

Fig. 6. Hydration age coefficient h for western Sierran slope sites, showing effects of variation of EHT with altitude; for surface conditions.

value of h_r from equation 13 with the EHT expression of equation 10, the suggested equations for the western slope of the Sierra Nevada are (with z being altitude above mean sea level in feet)

$t_{rcybp} = 103.09\ r^2 - 50, \quad z \le 1500$ ft (15a)

$t_{rcybp} = 56.71 \times \exp(0.00041z) \times r^2 - 50,$
1500 ft $< z < 4000$ ft (15b)

Figure 6 presents these data graphically.

The value of age coefficient h for the eastern slope of the Sierra, which scales from equation 13 by means of equation 14, presents an additional problem. Prior studies have shown that the EHT for the Bridgeport area is approximately 10°C (Rogers 2008b). Since equations 12 and 13 are for an EHT of 18.91°C, the temperature difference is 8.91°C; the exponential factor in equation 14 then has a value of 2.91, so the age equation for the eastern Sierra becomes

$t_{rcybp} = 300.31r^2 - 50$, for $0 \le r \le 8\mu$. (16)

The implications of this conclusion, in which the age coefficient seems much too large, are discussed below.

Discussion

The age equation for the western slope of the Sierra Nevada has been derived here to be

$t_{rcybp} = 103.09\ r^2 - 50, z \le 1500$ ft (15a)

$t_{rcybp} = 56.71 \times \exp(0.00041z) \times r^2 - 50,$
1500 ft $< z < 4000$ ft (15b)

where z is site altitude above mean sea level in feet. Rosenthal and Waechter (2002), based on a similar data set, proposed the equation

$t_{rcybp} = 149.05\ r^2 - 50,$ "below 914 m" (17)

This analysis predates temperature-dependent diffusion theory (Rogers 2007a), and the EHT analysis method was not described, nor is there any mention of depth correction. Furthermore, the altitude limit of 914 m corresponds to 3000 ft above mean sea level, not to the height of the meteorological inversion layer. As the hydration age coefficient is very sensitive to EHT, which in turn is very sensitive to meteorological conditions and to burial depth, the age coefficient in equation 17 must be treated with caution.

For eastern slope rates Rosenthal and Waechter proposed

$t_{rcybp} = 169.39\ r^2 - 50,$ "1820 to 2734 m"(18)

based on an analysis of time-sensitive projectile points. An alternative analysis of eastern slope rates by Rogers (2008d) yielded for an EHT of 9.83°C

$$t_{rcybp} = 177.59\ r^2 - 50, \quad \text{for } 0 \le r \le 7\mu. \quad (19)$$

which is comparable in magnitude to equation 18. The problem is that neither equation 18 nor 19 agrees with equation 16, where the age coefficient is 300.31 rcy/μ^2. There is no question that the age coefficient scales with EHT by equation 14; there is also no question that the EHT on the eastern slope is at least 6 - 9°C lower than on the western slope. Then by equation 14 the age coefficient on the eastern slope must be greater than on the west by a factor of 2 – 3, which is certainly not the case in comparing equations 18 and 19 with equation 16. This is a fundamental problem.

One way to assess realism of the age coefficients is to use Halford's 2002 data from the eastern slope (Halford 2002) and focus on Rose Spring projectile points. The advantage of Rose Spring points is that they were constrained to a fairly tight time interval, the Haiwee period. Yohe concluded that bow and arrow technology (including Rose Spring points) was well established at Rose Spring by 1600 BP (Yohe 1992, 1998). Similarly, it is generally agreed that Rose Spring point types were superseded by Desert and Cottonwood series by about 650 BP. The median for this interval is 1125 rcybp, or 1175 radiocarbon years corrected to 2000. Halford reported a sample of 11 Rose Spring points made of Bodie Hills obsidian, from known proveniences whose EHT could be assessed. The mean is $2.3 \pm 0.73\mu$. Computing the age coefficient from these data alone yields a value of 222.12 ± 84.36 yrs/μ^2, which is closer to the value in equation 16 than are the values in equation 18 or 19; if the point sample happened to be derived from a time earlier than the mid-point of the Haiwee period, the agreement is closer yet. However, if the age coefficient of equation 16 (300.31 yrs/μ^2) is used to compute the ages corresponding to Halford's projectile point hydration rim data, the ages are far too large, falling outside the expected age bands; even the Rose Spring rate of 222.12 yrs/μ^2 gives ages which are generally too large.

Conclusions

The errors inherent in the data set of Table 1 are evident, and are probably due to site formation processes which have introduced errors in the obsidian – radiocarbon associations. Equation 15 is usable, but the hydration age coefficients are probably no more accurate than ±25%, and chronometric analyses more fine-grained than this should not be attempted. For the eastern side of the Sierra Nevada, equation 19 is probably preferable, although again with the caveat that accuracy is no better than ±25%.

The data for each side of the Sierra Nevada yield internally-consistent rates and age coefficients. However, the age coefficients for eastern and western slopes are not consistent with each other when temperature scaling is taken into account. The western slope data reported in this paper, although fraught with problems arising from site formation processes, give an age coefficient which agrees to some degree with radiocarbon data. The eastern slope data reported elsewhere (Halford 2002; Rosenthal and Waechter 2002; Rogers 2008d) yield age coefficients which give consistent, although again equivocal, agreement with ages for temporally-sensitive projectile points in that area. However, the age coefficients on the two sides of the Sierra Nevada are not consistent with known temperature differences between the two regions. This issue cannot be resolved until better data on the chemistry, potential chemical variability, and possible rate variability of Bodie Hills obsidian are available.

Acknowledgements

This analysis would not have been possible without the encouragement of many people. I thank Kirk Halford, BLM archaeologist at Bishop, California, for first raising this fascinating problem. Jeff Rosenthal of Far Western Anthropological Research Group kindly provided data and the benefits of his long investigation of this problem. And I especially recognize my friend and colleague Chris Stevenson, whose vision of laboratory hydration as the best way to measure rates is well known; although I have deviated from his precepts here, I look forward to the day when they are fulfilled.

References Cited

Ambrose, W. R., and C. M Stevenson

2004 Obsidian Density, Connate Water, and Hydration Dating. *Mediterranean Archaeology and Archaeometry* 4(2):5-16.

Anovitz, Lawrence M., J. Michael Elam, Lee R. Riciputi, and David R. Cole

1999 The Failure of Obsidian Hydration Dating: Sources, Implications, and New Directions. *Journal of Archaeological Science* 26(7):735-752.

Carslaw, H. S., and J. C. Jaeger

1959 *Conduction of Heat in Solids*, 2nd ed. Oxford: Clarendon Press.

Cole, F. W.

1970 *Introduction to Meteorology*. Wiley: New York.

Crank, J.

1975 *The Mathematics of Diffusion*. Oxford: Oxford University Press.

Cvetanovic, R. J., D. L. Singleton, and G. Paraskevopoulos

1979 Evaluations of the Mean Values and Standard Errors of Rate Constants and their Temperature Coefficients. *Journal of Physical Chemistry* 83(1):50-60.

Doremus, R. H.

1994 *Glass Science*, 2nd ed. New York: Wiley-Interscience.

2000 Diffusion of Water in Rhyolite Glass: Diffusion-reaction Model. *Journal of Non-Crystalline Solids* 261 (1):101-107.

2002 *Diffusion of Reactive Molecules in Solids and Melts*. New York: Wiley Interscience.

Ebert, W. L., R. F. Hoburg, and J. K. Bates

1991 The Sorption of Water on Obsidian and a Nuclear Waste Glass. *Physics and Chemistry of Glasses* 34(4):133-137.

Friedman, Irving, Robert I. Smith, and William D. Long

1966 Hydration of Natural Glass and Formation of Perlite. *Geological Society of America Bulletin* 77:323-328.

Friedman, Irving, Fred W. Trembour, Franklin L. Smith, and George I. Smith

1994 Is Obsidian Hydration affected by Relative Humidity? *Quaternary Research* 41(2):185-190.

Gerald, C. F., and P. O. Wheatley.

1984 *Applied Numerical Analysis*, 3rd. ed. New York: Addison-Wesley.

Halford, F. K.

2002 *New Evidence for Early Holocene Acquisition and Production of Bodie Hills Obsidian*. Paper presented at the 28th Great Basin Anthropological Conference, Elko, NV.

Haller, W.

1963 Concentration-dependent Diffusion Coefficient of Water in Glass. *Physics and Chemistry of Glasses* 4(6):217-220.

Hull, Kathleen L.

2001 Reasserting the Utility of Obsidian Hydration Dating: A Temperature-Dependent Empirical Approach to Practical Temporal Resolution with Archaeological Obsidians. *Journal of Archaeological Science* 28:1025-1040.

Johnson, L. W., and R. D. Riess

1982 *Numerical Analysis*, 2nd ed. New York: Addison-Wesley

Mazer, J. J., C. M. Stevenson, W. L. Ebert, and J. K. Bates

1991 The Experimental Hydration of Obsidian as a Function of Relative Humidity and Temperature. *American Antiquity* 56(3):504-513.

Meyer, S.

1975 *Data Analysis for Scientists and Engineers*. Wiley: New York.

Onken, Jill

2006 *Effective Hydration Temperature and Relative Humidity Variation within the Nevada Test and Training Range, Southern Nevada*. Statistical Research Inc. Technical Report 06-50.

Ridings, Rosanna

1996 Where in the World Does Obsidian Hydration Dating Work? *American Antiquity* 61(1):136-148.

Rogers, Alexander K.

2007a Effective Hydration Temperature of Obsidian: A Diffusion-Theory Analysis of Time-Dependent Hydration Rates. *Journal of Archaeological Science* 34:656-665.

2007b Regional Scaling for Obsidian Hydration Temperature Correction. *Bulletin of the International Association for Obsidian Studies* 39: 15-23.

2008a Obsidian Hydration Dating and Relative Humidity: An Issue and a Suggested Protocol. *Bulletin of the International Association for Obsidian Studies* 38: 11-14.

2008b *Scaling of Temperature Data for EHT Computation: A Study of Sites near Bodie, California*. Maturango Museum Manuscript 41. Rev A dated 6 March 2008. Maturango Museum: Ridgecrest.

2008c Obsidian Hydration Dating: Accuracy and Resolution Limitations Imposed by Intrinsic Water Variability. *Journal of Archaeological Science*. 35:2009-2016.

2008d *A Method for Hydration Rate Estimation, with a Bodie Hills Example*. Maturango Museum Manuscript 44, dated 17 March 2008. Maturango Museum: Ridgecrest.

Rosenthal, Jeffrey S. and Sharon A. Waechter

2002 *Results of Phase-II Test Excavations at CA-ELD-616/H near Cool, Western El Dorado County.* Report prepared for CalTrans District 03, Marysville, California.

Stevenson, Christopher M., J. Carpenter, and B. E. Scheetz

1989 Obsidian Dating: Recent Advances in the Experimental Determination and Application of Hydration Rates. *Archaeometry* 31(2):1193-1206.

Stevenson, Christopher M., J. J. Mazer, and B. E. Scheetz

1998 Laboratory Obsidian Hydration Rates: Theory, Method, and Application. In: *Archaeological Obsidian Studies: Method and Theory. Advances in Archaeological and Museum Science*, Vol. 3, M. S. Shackley, ed., pp.181-204. New York: Plenum Press.

Stevenson, Christopher M., Mike Gottesman, and Michael Macko

2000 Redefining the Working Assumptions for Obsidian Hydration Dating. *Journal of California and Great Basin Anthropology* 22(2):223-236.

Stevenson, Christopher M., Ihab. M. Abdelrehim, and Steven W. Novak

2004 High Precision Measurement of Obsidian Hydration Layers on Artifacts from the Hopewell Site Using Secondary Ion Mass Spectrometry. *American Antiquity* 69(4):555-568.

Van Huffel, S., and J. Vandewalle

1991 *The Total Least Squares Problem: Computational Aspects and Analysis*. Society for Industrial and Applied Mathematics: Philadelphia.

Wagner, Carl

1950 Diffusion of Lead Chloride Dissolved in Solid Silver Chloride. *Journal of Chemical Physics* 18(9): 1227-1230.

Yohe, R. M. II

1992 *A Reevaluation of Western Great Basin Cultural Chronology and Evidence for the Timing of the Introduction of the Bow and Arrow to Eastern California based on new Excavations at the Rose Spring Site (CA-INY-372).* Unpublished PhD Dissertation, Department of Anthropology, University of California, Riverside.

1998 The Introduction of the Bow and Arrow and Lithic Resource Use at Rose Spring (CA-INY-372). *Journal of California and Great Basin Anthropology* 20(1):26-52.

Zhang, Youxue, E. M. Stolper, and G. J. Wasserburg

1991 Diffusion of Water in Rhyolitic Glasses. *Geochimica et Cosmochimica Acta* 55(2):441-456.

ABOUT OUR WEB SITE

The IAOS maintains a website at http://www.peak.org/obsidian/
The site has some great resources available to the public, and our webmaster, Craig Skinner, continues to update the list of publications and must-have volumes.

You can now become a member online or renew your current IAOS membership using PayPal. Please take advantage of this opportunity to continue your support of the IAOS.

Other items on our website include:

- World obsidian source catalog
- Back issues of the *Bulletin.*
- An obsidian bibliography
- An obsidian laboratory directory
- Photos and maps of some source locations
- Links

Thanks to Craig Skinner for maintaining the website. Please check it out!

CALL FOR ARTICLES

Submissions of articles, short reports, abstracts, or announcements for inclusion in the *Bulletin* are always welcome. We accept electronic media on CD in MS Word. Tables should be submitted as Excel files and images as .jpg files. Please use the *American Antiquity* style guide (available at www.saa.org/publications/StyleGuide/styFrame.html) for formatting references and bibliographies.

Submissions can also be emailed to the *Bulletin* at cdillian@coastal.edu Please include the phrase “IAOS Bulletin” in the subject line. An acknowledgement email will be sent in reply, so if you do not hear from us, please email again and inquire.

Deadline for Issue #44 is November 1, 2010.

Send submissions to:

Carolyn Dillian
IAOS *Bulletin* Editor
c/o Center for Archaeology and Anthropology
Department of History
Coastal Carolina University
P.O. Box 261954
Conway, SC 29528
U.S.A.

Inquiries, suggestions, and comments about the *Bulletin* can be sent to cdillian@coastal.edu Please send updated address information to Colby Phillips at colbyp@u.washington.edu

MEMBERSHIP

The IAOS needs membership to ensure success of the organization. To be included as a member and receive all of the benefits thereof, you may apply for membership in one of the following categories:

Regular Member: $20/year*
Student Member: $10/year or FREE with submission of a paper to the *Bulletin* for publication. Please provide copy of current student identification.
Lifetime Member: $200

Regular Members are individuals or institutions who are interested in obsidian studies, and who wish to support the goals of the IAOS. Regular members will receive any general mailings; announcements of meetings, conferences, and symposia; the *Bulletin*; and papers distributed by the IAOS during the year. Regular members are entitled to vote for officers.

*Membership fees may be reduced and/or waived in cases of financial hardship or difficulty in paying in foreign currency. Please complete the form and return it to the Secretary-Treasurer with a short explanation regarding lack of payment.

NOTE: Because membership fees are very low, the IAOS asks that all payments be made in U.S. Dollars, in international money orders, or checks payable on a bank with a U.S. branch. Otherwise, please use PayPal on our website to pay with a credit card. http://www.peak.org/obsidian/

For more information about the IAOS, contact our Secretary-Treasurer:

Colby Phillips
IAOS
c/o University of Washington
Department of Anthropology
Box 353100
Seattle, WA 98195-3100
U.S.A.
colbyp@u.washington.edu

Membership inquiries, address changes, or payment questions can also be emailed to colbyp@u.washington.edu

ABOUT THE IAOS

The International Association for Obsidian Studies (IAOS) was formed in 1989 to provide a forum for obsidian researchers throughout the world. Major interest areas include: obsidian hydration dating, obsidian and materials characterization ("sourcing"), geoarchaeological obsidian studies, obsidian and lithic technology, and the prehistoric procurement and utilization of obsidian. In addition to disseminating information about advances in obsidian research to archaeologists and other interested parties, the IAOS was also established to:

1. Develop standards for analytic procedures and ensure inter-laboratory comparability.
2. Develop standards for recording and reporting obsidian hydration and characterization results
3. Provide technical support in the form of training and workshops for those wanting to develop their expertise in the field
4. Provide a central source of information regarding the advances in obsidian studies and the analytic capabilities of various laboratories and institutions.

MEMBERSHIP RENEWAL FORM

We hope you will continue your membership. Please complete the renewal form below.

NOTE: You can now renew your IAOS membership online! Please go to the IAOS website at http://www.peak.org/obsidian/ and check it out! Please note that due to changes in the membership calendar, your renewal will be for the next calendar year. Unless you specify, the *Bulletin* will be sent to you as a link to a .pdf available on the IAOS website.

___ Yes, I'd like to renew my membership. A check or money order for the annual membership fee is enclosed (see below).

___ Yes, I'd like to become a new member of the IAOS. A check or money order for the annual membership fee is enclosed (see below). Please send my first issue of the IAOS *Bulletin*.

___ Yes, I'd like to become a student member of the IAOS. I have enclosed either an obsidian-related article for publication in the IAOS *Bulletin* or an abstract of such an article published elsewhere. I have also enclosed a copy of my current student ID. Please send my first issue of the IAOS *Bulletin.*

NAME: ____

TITLE: ________________________ AFFILIATION:_______________________________

STREET ADDRESS: ____

CITY, STATE, ZIP: ____

COUNTRY: ____

WORK PHONE: ______________________________ FAX: _________________________

HOME PHONE (OPTIONAL): ____

EMAIL ADDRESS: ____

My check or money order is enclosed for the following amount (please check one):
___ $20 Regular
___ $10 Student (include copy of student ID)
___ FREE Student (include copy of article for *Bulletin* and student ID)
___ $200 Lifetime

Please return this form with payment to:
Colby Phillips
IAOS
c/o University of Washington
Department of Anthropology
Box 353100
Seattle, WA 98195-3100
U.S.A.